REPORT DOCUMENTATION PAGE	Form Approved OMB No. 0704-0188

Public reporting burden for this collection of information is estimated to average 1 hour per response, including the time for reviewing instructions, searching existing data sources, gathering and maintaining the data needed, and completing and reviewing the collection of information. Send comments regarding this burden estimate or any other aspect of this collection of information, including suggestions for reducing this burden, to Washington Headquarters Services, Directorate for Information Operations and Reports, 1215 Jefferson Davis Highway, Suite 1204, Arlington, VA 22202-4302, and to the Office of Management and Budget, Paperwork Reduction Project (0704-0188), Washington, DC 20503.

1. AGENCY USE ONLY (Leave blank)	2. REPORT DATE 5/30/95	3. REPORT TYPE AND DATES COVERED Final Report: 4/3/92 to 3/31/95

4. TITLE AND SUBTITLE	5. FUNDING NUMBERS
A Critical Study of Constitutive Relations for Finite Strain Inelasticity	DAAL03-92-G-0103

6. AUTHOR(S)

David L. McDowell, Professor
G.W. Woodruff School of Mechanical Engineering

7. PERFORMING ORGANIZATION NAME(S) AND ADDRESS(ES)

Georgia Tech Research Corporation
Georgia Institute of Technology
Atlanta, GA 30332-0420

8. PERFORMING ORGANIZATION REPORT NUMBER

9. SPONSORING/MONITORING AGENCY NAME(S) AND ADDRESS(ES)

U. S. Army Research Office
P. O. Box 12211
Research Triangle Park, NC 27709-2211

10. SPONSORING/MONITORING AGENCY REPORT NUMBER

ARO 29543.16-EG

11. SUPPLEMENTARY NOTES

The view, opinions and/or findings contained in this report are those of the author(s) and should not be construed as an official Department of the Army position, policy, or decision, unless so designated by other documentation.

12a. DISTRIBUTION/AVAILABILITY STATEMENT	12b. DISTRIBUTION CODE
Approved for public release; distribution unlimited.	

13. ABSTRACT (Maximum 200 words)

An unique set of experiments has been conducted to study the response of three FCC alloys to abrupt changes of loading direction at finite strain using large strain compression and torsion experiments, as well as sequences of the two. Evolution of grain morphology, substructure and texture have been experimentally quantified. It was observed that in spite of differences in dislocation substructures and mechanisms of inelastic deformation, the nonproportional straining response of the two alloys which exhibited homogeneous deformation at the macroscale, type 304L stainless steel and OFHC Cu, was very similar.

These experiments and complementary modelling effort have led to improved understanding of the relative roles of dislocation substructure and texture development in establishing anisotropy of the flow stress. Neither state-of-the-art internal state variable theories for finite inelasticity which employ only plastic spin to account for textural anisotropy or polycrystal continuum slip plasticity models which employ the Taylor assumption of uniform deformation gradient among grains are able to correlate the observed behavior. A macroscale internal state variable model was developed to address the anisotropic hardening associated with dislocation substructure development and texturing, consistent with experimental observations and with the physics of deformation processes. The model has been generalized to viscoplasticity with void growth effects. The program has extensively leveraged the ARO funds to achieve comprehensive objectives through interaction with Sandia National Laboratories in Livermore, CA.

14. SUBJECT TERMS			15. NUMBER OF PAGES
	DTIC QUALITY INSPECTED 3		16. PRICE CODE

17. SECURITY CLASSIFICATION OF REPORT	18. SECURITY CLASSIFICATION OF THIS PAGE	19. SECURITY CLASSIFICATION OF ABSTRACT	20. LIMITATION OF ABSTRACT
UNCLASSIFIED	UNCLASSIFIED	UNCLASSIFIED	UL

NSN 7540-01-280-5500

Standard Form 298 (Rev. 2-89)
Prescribed by ANSI Std. Z39-18
298-102

DTIC
ELECTE
JUL 10 1995
B

Final Report

A CRITICAL STUDY OF CONSTITUTIVE RELATIONS
FOR FINITE DEFORMATION INELASTICITY

Principal Investigator/Project Director
David L. McDowell, Professor
George W. Woodruff School of Mechanical Engineering
Georgia Institute of Technology
Atlanta, GA 30332-0405

May 1995

OVERVIEW AND SPECIFIC AIMS OF PROGRAM

The use of crystal plasticity concepts to qualitatively and, in some cases, quantitatively correlate texture development at finite strain has been a promising development of the last decade. However, it is becoming increasingly clear that complex low energy dislocation structures (LEDS) form in response to imposed finite deformations to accommodate slip; examples include geometrically necessary boundaries and microbands. These features are not equivalent to shear bands as they represent immobile dislocation structures which serve to inhibit slip. Moreover, these structures are not incorporated naturally within continuum slip polycrystal plasticity theory or conventional macroscale plasticity theory, yet play a first order role in the development of apparent textural anisotropy. Recent studies suggest that both bcc and fcc crystal structures have in common the development of certain characteristic orientations and intensities for these LEDS.

The goals of this three-year research program were to:

(1) better understand the relative roles of dislocation substructure and texture development in establishing anisotropy of the flow stress;

(2) conduct a set of critical experiments for three distinctly different fcc metals involving finite strain compression, torsion and sequences of compression-compression, compression-torsion and torsion-tension;

(3) develop a macroscale constitutive model for the anisotropic hardening associated with dislocation substructure development and texturing, consistent with experimental observations and with the physics of deformation processes.

In this report, we summarize how these goals have been addressed by a productive

effort which has led to basic developments in (i) quantifying the stress state dependence and stress state sequence effects on the mechanical behavior and grain/substructure morphology of several different FCC polycrystals based on large strain compression, finite torsion of thin-walled tubes and sequential compression-torsion tests, and (ii) a macroscale plasticity model based on internal state variables which accounts for dislocation substructure effects in both the yield function and hardening rules. The program has extensively leveraged the ARO funds to achieve comprehensive objectives through interaction with Sandia National Laboratories in Livermore, CA along with matching funds from Georgia Tech.

RESULTS

The original proposal outlined six tasks. This research program has completed each of these tasks, resulting in significant findings and novel modelling concepts. We briefly present these here, along with summaries of key related research findings.

(i) *conduct critical experiments*
  * A complete set of unique finite strain experiments have been conducted in this program, including compression, torsion, and sequences of compression-torsion, torsion-tension, etc. (Miller, 1993; Graham, 1995). In addition to optical microscopy (Lustig, 1995), x-ray diffraction measurement of texture has been conducted in a companion AASERT project (G. Butler, graduate student). The mechanical testing program is sufficiently unique that it was selected as a finite strain database in a recent NSF workshop on this subject.

(ii) *study the role of the ratio of kinematic to isotropic hardening*
  * It was found that for realistic levels of kinematic hardening (approximately 10-20% of the flow stress), secondary axial effects in finite strain shear can be reasonably correlated along with the first order shear stress versus plastic shear strain (Miller & McDowell, 1992; Miller, 1993; Miller & McDowell, 1995).

(iii) *consideration of forms other than J_2 theory for anisotropic work hardening*
  * The third invariant of deviatoric overstress, J_3^*, was introduced in addition to the second invariant to better capture the effects of stress state dependence of multislip constraint in both the yield function and hardening laws of internal state variables in a macroscale formulation of flow and hardening rules (Miller, 1993; Graham, 1995).

(iv) *study behavior under conditions of loading direction change after finite prestrain, both short and long range transients*
  * The mechanical tests involved abrupt load direction changes after finite prestrain; accordingly, the modelling effort has addressed the subsequent behavior shortly after the change as well as the long range, asymptotic nature of the flow stress (Miller, 1993; Miller & McDowell, 1994, 1995).

(v) *study the significance of plastic spin*
  * Through consideration of the first order stress-strain behavior, axial extension

during free-end shear with and without finite compressive prestrain, and physically appropriate nonlinear kinematic hardening forms along with a realistic saturation level for the kinematic hardening variable(s), it was determined that the magnitude of plastic spin necessary to achieve correlation was substantially lower than that corresponding to J_2 theory with pure kinematic hardening (cf. Miller, 1993; Miller & McDowell, 1995). This is in accordance with the physical observation that the rate of texture evolution (grain rotation) is actually substantially lower than that indicated by the neglect of grain sub-division (microtexturing) by assumption of a uniform deformation gradient among grains (Taylor model). Evolving grain substructure plays the role of relaxing constraints among grains, thereby reducing the rate of plastic spin relative to the common phenomenological idealization of continuum slip polycrystal plasticity (Horstemeyer, 1995).

(vi) *examine the role of noncoaxiality of stress and plastic strain rate on induced anisotropy*
    * Through the efforts cited in item (iv) above, the observed effects of noncoaxiality have been addressed in two ways. First, the introduction of J_3^* dependence of the kinematic and isotropic hardening affect the long range transient behavior. Second, the incorporation of scalar products of the backstress and direction of inelastic flow in the internal variable hardening rate equations, along with memory of the maximum level of constraint, affect the short range transients (Miller & McDowell, 1995).

In the following sections, we provide more detail concerning these results.

I. Experimental Program

In this program, a *very unique* set of finite strain experiments were conducted at room temperature and an effective strain rate on the order of 4×10^{-4} s^{-1}. The experiments were designed to examine:

1. The path dependence of stress-strain response and associated deformation substructure morphology/textures for sequences of compression and torsion, and orthogonal compression-compression loading.
2. The nature of anisotropy following finite prestrain, based on the transition between applied stress states, asymptotic behaviors, small nonproportional cyclic strain histories and second order axial extension during shear with and without prestrain.
3. The development of texture and deformation substructure morphology and its relation to cumulative plastic strain for different stress states.

Three distinct FCC alloys were investigated, including 304L stainless steel, 6061-T6 Al and OFHC Cu. Stainless steel 304L has very low stacking fault energy and dislocation substructures are formed in accordance with Taylor slip (planar glide) processes. The Al alloy exhibits dislocation cell structures, while the Cu is intermediate. Considerable finite strain data (particularly torsion) exists on the OFHC Cu, although the data are highly

dependent upon initial grain size and heat treatment. Sandia National Laboratories has experience in testing both the 304L and 6061-T6 materials, while we have drawn upon the experience of Los Alamos National Laboratory to define the appropriate heat treatment and initial condition for the Cu in order to achieve consistency with their data.

The mechanical testing and optical microscopy studies was completed for all three materials. The data for 304L SS and OFHC Cu are considered to be most appropriate for model development as they correspond to a reasonably high degree of uniformity of deformation in the gage section of specimens at the deformation levels considered for both stress states. The 6061-T6 Al exhibited early localization in shear due to its weak strain hardening character; this data may be of use in assessing or developing models for shear banding and its effects on structural response.

This experimental program has been adopted as an international benchmark program at a recent workshop sponsored by the U.S. National Science Foundation to permit constitutive model developers around the world to evaluate their finite strain constitutive models on a normative basis. The thesis of Samuel Graham provides a thorough description of these results to interested researchers, and APPENDIX A summarizes key results which reside on a 3.5" dos-formatted floppy disk with ASCII data files. Experiments include compression, torsion and compression-torsion sequence experiments for 304L stainless steel, 6061-T6 Al and OFHC Cu at room temperature. It is one of the most complete, self-contained datasets of its kind that is accessible within the public domain. Figures 1-3 summarize the results of mechanical tests for all three materials.
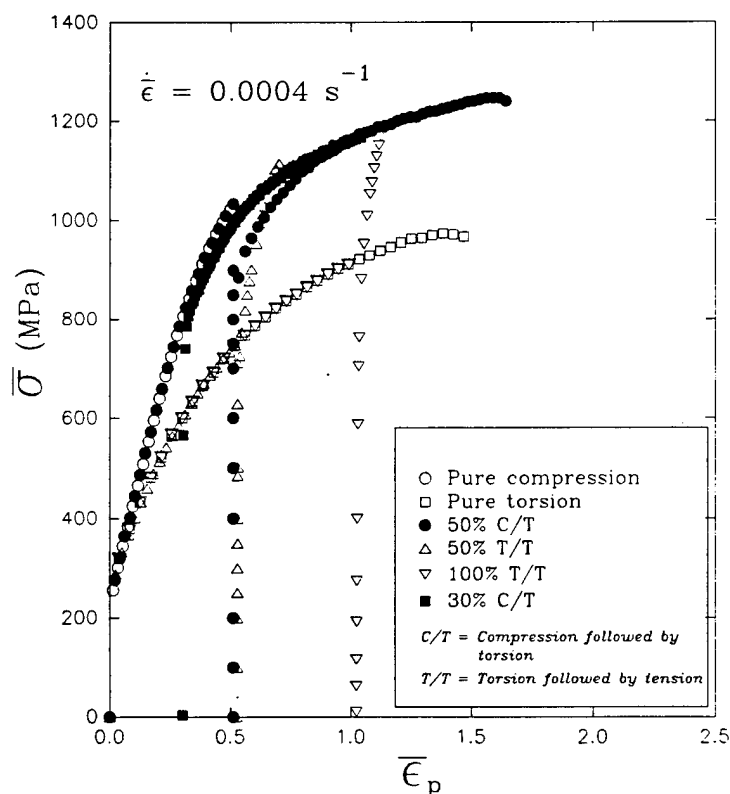

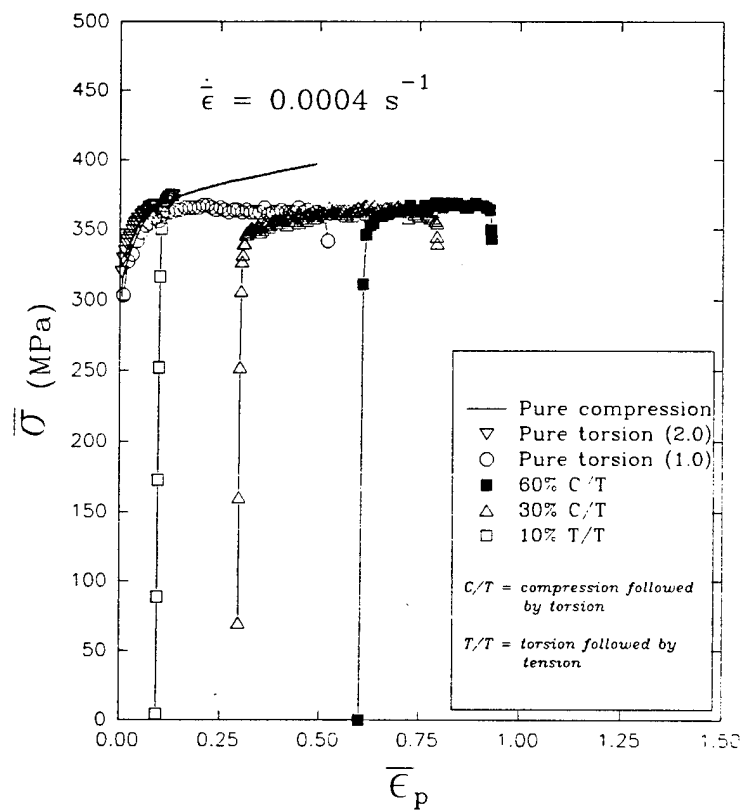Figure 1   Effective stress versus plastic strain for 304L stainless steel

Figure 2   Effective stress versus plastic strain for 6061-T6 Al.
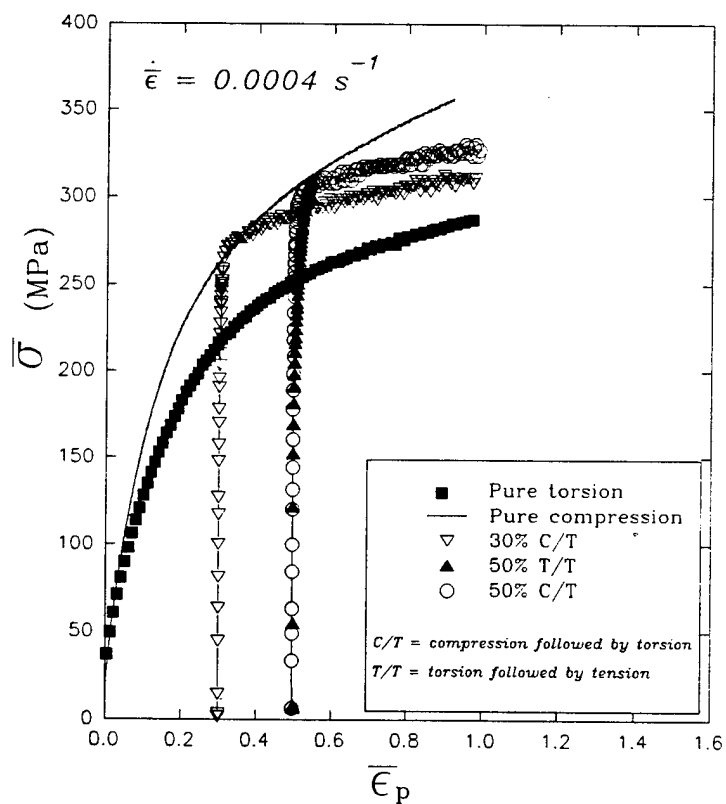

Figure 3   Effective stress versus plastic strain for OFHC Cu.

Optical microscopy measurements have been performed on specimens to gain information regarding deformation structures and grain morphology, as reported principally in the thesis of Steven Lustig (1995). Texture measurement is the focus of an accompanying AASERT program, undertaken by Mr. G. Butler.

Two aspects of the experimental program are particularly important. First, the focus was on the moderate ($< 100\%$) strain regime where development of both dislocation substructure and texture is in formative stages. This regime provides perhaps the most interesting challenges to development of constitutive equations. Second, these challenges are most clearly highlighted by experiments involving sequences of finite straining under different stress states. Due to the difficulty inherent in maintaining homogeneous (or nearly so) deformation at finite strain in compression or shear, such experiments demand a great deal of care, technique development and expertise.

To first order, the strain was maintained as either shear or compressive until switching to the other state after predominately elastic unloading. These simple types of paths are most illustrative of the interaction between microstructural level features which develop differently in compression and shear. In contrast to yield surface probing experiments, the subsequent shear or compression/tension is applied well into the regime of inelastic deformation to assess the work-hardening interactions rather than just the effect on subsequent initial yield behavior (very small offset plastic strains) after elastic unloading.

As previously mentioned, a relative softening in torsion is typically observed relative to tension using effective stress defined on the basis of J_2. This softening effect is observed coincidentally with the formation of dislocation substructure which is quite distinct in orientation from that observed in either tension or compression (cf. Hughes and Nix, 1989; Hughes and Hansen, 1991). While sometimes referred to as textural softening, the anisotropy associated with texture processes is not yet fully developed at the moderate strain levels examined here and dislocation substructure plays a comparable role. Although a large number of tension, compression and torsional experiments exist, very few experiments have been conducted which involve sequences of stress states, each carried out to finite strain where texture development is well underway. Two questions were of interest in the experimental program. The first was whether the stress-strain response and associated dislocation substructures/textures are strongly path dependent or largely reversible through sequences of loading. The second is the extent to which stress-strain response is linked to the observed texture formation. The data generated in this project provides significant insight into the first question, while that of the ongoing AASERT program is largely addressing the second.

Fundamentally, there are several issues related to changing stress state after finite prestrain. One issue is whether or not the response approaches, either asymptotically or rapidly, the stress-strain behavior observed for loading from the virgin condition with the current stress state (e.g. compression or shear). Another issue is the precise nature of the transition from one stress state to another, and whether this transition can be described on the basis of the hardening laws and the flow potential. Complete transition from prior compression to the shear response observed for virgin, unstrained material, for example, may indicate a certain reversibility of dislocation substructure, depending on the rate of the transition. A lack of complete transition of this sort may indicate permanent, irreversible substructural anisotropy associated with the yield function and possibly with short range

kinematic hardening variables. In general, the experimentally observed magnitude of differences between flow stresses in shear and compression at large strains combined with the thermodynamical constraint that the backstress should not exceed about 10% of the flow stress require that both the yield function and the hardening rules exhibit the effects of dislocation substructure development with cumulative deformation, since convexity of the yield function must be preserved. Since the evolution of dislocation substructure is most likely reflected by a gradual transition of the flow stress after a change of loading condition, the hardening rules are the most logical primary repository for this behavior.

The compression experiments were carried out at Sandia-Livermore with a high degree of homogeneous deformation. An intensive effort of experimental iteration concerning different lubrication and end-grooving arrangements preceded this program at SNL. Tubular Lindholm specimens were then machined from compressively prestrained or virgin material, and free-end (axially unconstrained) torsion tests are performed at Georgia Tech.

In torsion, the 6061-T6 Al alloy exhibited the onset of shear localization at the center of the gage section at strains on the order of 10%; at shear strains on the order of 20-40%, this localization was pronounced due to the weak strain hardening character of this material. Hence, the 6061-T6 Al behavior is considered perhaps useful for localization studies, but not for basic understanding of deformation behavior which should be macroscopically homogeneous to first order. On the other hand, both the 304L stainless steel (Miller, 1993) and the OFHC Cu materials (Graham, 1995) exhibited uniform shear deformation in the gage section (over 90% within the gage section) due to the high workhardening rates of these two materials, as determined by etched longitudinal lines. Several generic comments pertain to the results which appear in Figures 1 and 3 for both the 304L and OFHC Cu materials:

(i) The J_2 effective flow stress in compression is elevated considerably above that of torsion (approximately 25% higher).

(ii) Upon unloading from compression at true strains on the order of 50% to 100% and switching to torsion, most of the accumulated hardening is retained; the work-hardening rate is initially much higher (short range transient) than that for torsion at the same effective strain level, but transitions within additional effective strain of 50% to 100% to essentially the same hardening rate as pure torsion (long range transient). However, the effective flow stress is nearer that of compression than torsion in this case.

(iii) Upon unloading from torsion at large strain and switching to tension, a dramatic increase in the workhardening rate is observed and the effective flow stress tends rapidly toward that of pure compression. The transition is made within approximately 10% subsequent cumulative plastic strain in tension. The conclusion drawn from these experiments is that the hardening imparted during the initial straining has a permanent effect on the material hardening characteristics and effective flow stress.

Of course, the deformation mechanisms of 304L SS and OFHC Cu are completely different. The former undergoes a deformation-induced martensitic transformation along with deformation twinning and predominately planar slip. Some interesting aspects of these mechanisms for 304L SS are described by Miller (1993) and Miller & McDowell (1995). An

interesting finding is that of an increased α' martensite production in compression compared to torsion, likely resulting from a higher density of nucleation sites in compression.

In contrast, OFHC Cu did not exhibit significant transformation or deformation twinning processes. In view of these differences, the similarity of features of mechanical behavior in Figures 1 and 3 are remarkable. Moreover, data reported by Hecker and Stout (1984) on 70-30 brass exhibits very similar behavior to that of these materials without the same set of apparent irreversible mechanisms or degree of texturing. This may be related to the fact that grain sub-division and the generation of features such as geometrically necessary dislocation boundaries (LEDS) evolve in a very similar manner for different fcc polycrystals as well as bcc structures. Clearly, it may be also hypothesized that first order textural anisotropy (i.e. mean texture) plays a role in analogous behavior, although our recent polycrystal plasticity studies (Butler, 1995; Horstemeyer, 1995) suggest that texture evolution along cannot reflect these generic features of mechanical behavior. The macroscale modelling effort described later seeks to address these common behaviors, and appropriate modifications of polycrystal plasticity theory are underway.

In this program a technique was developed using a capacitance transducer to measure the axial extension of free-end torsion specimens with high accuracy, resolution and repeatability. In Figures 4-5, the induced axial strain is plotted as a function of shear strain for both the pure torsion test and for the torsion episode of the compression/torsion sequence test for both 304 SS and OFHC Cu. The induced axial strain appears to be independent of compressive prestrain for 304L SS, but not so for OFHC Cu.
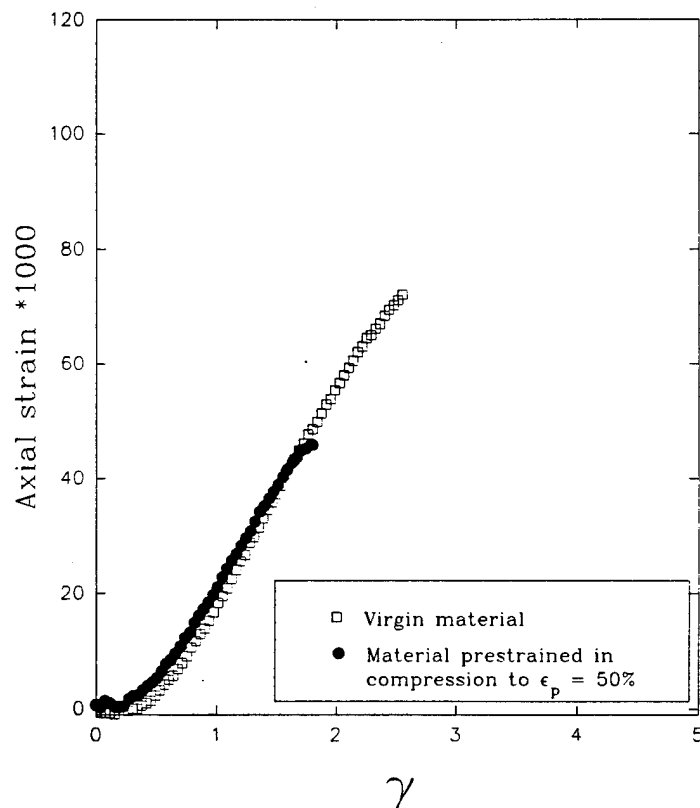

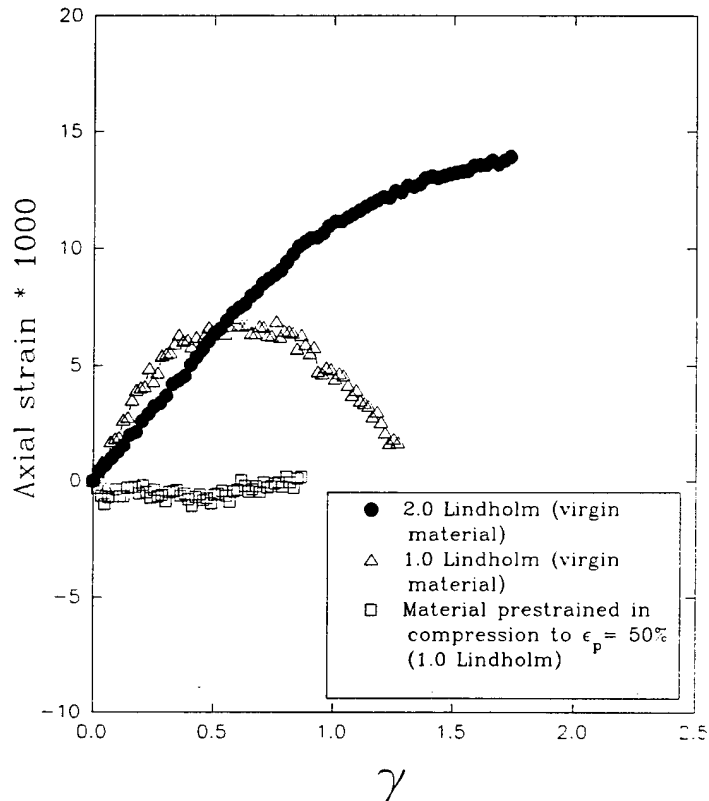Figure 4   Axial extension during free-end shear of 304L SS.

Figure 5   Axial extension during free-end shear of OFHC Cu.

In general, we observed differences in the axial extension responses of small and large Lindholm specimens for both 304L and OFHC Cu, although the first order effective stress versus effective plastic strain were the same given the same initial condition. This may be attributed to fewer grains across the wall thickness of the small (1" Lindholm specimens) and associated differences in distribution of flow, as well as perhaps the distribution of plasticity outside the gage section. Such data, presented in the thesis of S. Graham (1995) may be of considerable value to polycrystal plasticity modelling efforts to discern grain size effects relative to structural dimensions.

In addition to the compression-torsion and torsion-tension experiments, a series of compression-compression experiments were performed on all three materials. In this case, cylindrical test specimens were compressed to approximately 50% true strain at each stage, then re-machined into smaller cylindrical specimens with axis perpendicular to that of the original compression. This was repeated in some cases up to 200% strain, keeping track of the sequential compression axes. The data for this test program are still under analysis, and will be reported in forthcoming work of M. Horstemeyer and G. Butler. It provides an additional set of nonproportional straining experiments at finite strain which will be of use

in evaluating the performance of both macroscale and microscale plasticity models.

Texture Measurement:

Since texture development is one of two principal sources of the deformation-induced anisotropy at finite strain, an important ancillary aspect of the experimental program is the quantification of texture at different stages of finite deformation and for different stress states. This has been performed in collaboration with an AASERT award which has been underway since Fall 1993, with an experimental focus on:

(1) development of specialized mounting techniques to obtain approximate pole figure representations of mean textures (rather than microtextures) for the thin-walled tubular specimen geometries,

(2) X-ray diffraction pole figure measurements on the 304L SS and OFHC Cu in the virgin state, after prior compression, and after sequences of compression/torsion, and

(3) development of different techniques for presenting pole figures and filtering data appropriately, including the popLA code from Los Alamos National Laboratory and an in-house plotting routine (AXUM).

Samples were cut to expose the transverse plane (i.e. the plane perpendicular to the cylinder axis) or the longitudinal-radial plane (i.e. the plane containing the cylinder's central axis); these two orientations used with each (hkl) and deformation state are sufficient to allow reconstruction of most of the pole figure, in practice, using a reflection-type instrument.

A technical graphics package, AXUM, was purchased in order to replace plotting routines previously used for outputting pole figures (the proprietary plotting software was for a mainframe system which no longer exists). The FORTRAN code for transforming the raw data into coordinates on the stereographic projection was altered to run on a PC, and standardized procedures in AXUM have been developed for plotting pole figures from the experimental data.

The pole figure diffractometer is configured to operate in the Schulz setting (Cullity, 1978), and accurate intensity measurements in reflection are limited to X-angles greater than 20 or 25 degrees. Outside this angular range, corrections for geometry are generally too imprecise to be reliable; typically one studies the material in transmission to complete the outer portions of the pole figure. As this is impractical in the present instance (see below), the experimental pole figures can be completed by cutting samples along a plane or planes orthogonal to the original surface and by recording these additional pole figures. While this is a rather laborious process, it provides a higher degree of reliability than methods which fill in the pole figure by extrapolating from the known intensity distribution.

The apparatus currently uses a chromium target; we have found that background is substantially reduced compared to that obtained with a copper x-ray tube and this improves the quality of the texture data. Given the quite low penetrability of Cr K α radiation and the quite high absorptivity of steel, it is impractical to do transmission texture measurements. The same consideration also holds for Ag and Mo sources which provide the most penetrating characteristic radiation of any commercially available x-ray tubes.

The 111, 200 and 220 pole figures from two orientations are being measured for each sample. The first orientation is with the sample surface cut normal to the compression axis; this is termed the transverse orientation. The second orientation is along a plane parallel to the compression axis, i.e., a longitudinal orientation. In the thin-walled tubular specimens, there are two orientations of the longitudinal planes which reflect the geometry of the tube. Longitudinal planes cut at 90 degrees to the samples' walls (and passing through the center of the tube) are termed longitudinal-radial specimens while those samples cut along a tangential plane in the cylinder wall are identified as being in the longitudinal-tangential orientation. Both the longitudinal-radial orientation and the transverse orientations are being studied.

Because of the small cross-sectional area of the tubular samples and the fact that, even with an irradiated area of only several square millimeters, the irradiated area varies with angle on the pole figure, collecting unbiased data requires cutting the sample into numerous small sections and placing the pieces side-by-side in identical orientations. The pieces are then mounted in cold mount, and the surface to be studied with x-ray diffraction is metallographically prepared. These "composite" samples are analogous to samples constructed for measuring texture in wires with a diffractometer. Note that two separate composite samples (transverse and longitudinal-radial) must be made from the material with a given loading history. Most of the samples for which pole figures have been obtained in one orientation and not in the second, are mounted in the second orientation ready for the pole figure determination.

We obtained the Preferred Orientation Package from Los Alamos National Laboratory (popLA) and have implemented its routines for determining and plotting orientation distribution functions and for plotting pole figures. Both the popLA routines and those developed with AXUM will be employed for plotting the pole figures, but the low order gray scale images offered by the former are relatively easy to visually interpret.

To date, pole figures have been obtained for most of the key experiments on both 304L stainless steel and OFHC Cu. Both undeformed material and material from specimens available at several discrete stages of the multistep deformation process have been quantified for development of texture. Examples of the multistage deformation processes include sequential large strain compression with re-machining followed by finite shear, finite shear to several strain levels and finite shear followed by tension. Smooth cylindrical specimens were used for compression experiments, while Lindholm or modified-Lindholm specimens were used for torsion. In both cases, the deformation may be regarded, to first order, as homogeneous.

Pole figures have been generated in both AXUM (detailed data representation) and popLA (averaged representation) formats for both sample orientations for all of the steel samples measured. Software was written to convert our data measurement format into one that would be compatible with popLA, and this software was used to create the popLA pole figures. This software was further modified to allow for normalizing the data to a random sample (for a "times random" stereographic projection) and to permit adjustment by correction factors to account for measurement deviations due to the apparatus itself (e.g. geometrical variation of the area of the sample illuminated by the beam). These correction factors have been calculated, and are being applied to selected sample measurements for evaluation. Eventually, they will be imposed on all of the texture measurements.

Many of the literature references plot stereographs from a different specimen direction (e.g. radial versus our longitudinal or tangential), so new software was written to facilitate rotation of the pole figures plotted in AXUM. In this manner we were able to verify the consistency of our data with those in the existing literature for pure compression and torsion. This software has been further upgraded to include the option to normalize the data and apply correction factors, as described above. Several pole figures have been recorded for two reference samples, rolled copper and recrystallized copper. These samples were studied in order to be sure the apparatus was functioning correctly and that the new plotting routines were accurate and in order to provide baseline data with which to compare results obtained after the PC-control and modernization are complete. The 111 and 200 pole figures for the rolled copper sample are the same as pole figures which appear in the literature (e.g., Thompson et al, 1989).

Of particular value, both to this program and to other researchers, will be the presentation of texture data, in the form of pole figures, side-by-side with mechanical stress-strain behavior for various finite strain loading paths. Such a presentation will facilitate improved understanding of the coupling of texture evolution with mechanical behavior. The evolution of texture following a change of loading path direction is particularly interesting. Following compressive prestrain, for example, the compression texture evolves in a significant manner during subsequent shear towards a shear texture, although it develops much more weakly than might be anticipated based on the equivalent plastic strain level involved.

It is expected that in the coming 6-12 months, several papers will be written which comprehensively present mechanical behavior along with pole figures to draw conclusions regarding modelling of polycrystalline behavior.

II. Model Development

Macroscale:

The objective of the modelling effort was to develop a macroscale plasticity framework which addresses experimentally observed aspects of anisotropy, placing the role of textural anisotropy in its proper perspective among other potential contributions to anisotropic workhardening such as formation of dislocation microbands and microstructural transformations. Within the context of incompressible finite strain plasticity, the role and interpretation of the third invariant of the deviatoric overstress, J_3^*, has been a focal point of this work, in the context of combined kinematic-isotropic hardening. Accordingly, items (ii), (iii), (v) and (vi) on pages 2-3 have been thoroughly addressed in the experimentally-motivated modelling program (cf. theses of Miller, 1993; Graham, 1995; Lustig, 1995).

Inclusion of J_3^* accounts for dislocation substructure effects in both the yield function and hardening rules for kinematic and isotropic internal state variables. These modifications permit correlation of both finite strain compression as well as finite simple shear. The framework addresses secondary effects such as development of axial strain in unconstrained (zero axial load) simple shear and development of axial stress in constrained (zero axial displacement) simple shear of tubular specimens.

Dominant inelastic deformation processes of metal polycrystals at large strain include

the nucleation and evolution of dislocation substructures, deformation twinning, phase transformations, and the evolution of crystallographic texture. Due to its technological importance, crystallographic texture has been the focus of much of the current research in large strain. Strain-hardening theories which incorporate deformation substructure, such as the mesh length theory of Kuhlmann-Wilsdorf (1962, 1983), have been largely ignored in large strain deformation model development, however. Accounting for strain-hardening processes either directly in the case of microscale models or indirectly in the case of macroscale models is necessary for a more complete theory.

The mesh length theory proposes that clusters of stress-screened dislocation arrays, which are lower energy structures than uniform or statistically predictable distributions, will prevail (Hansen & Kuhlmann-Wilsdorf, 1986). These clusters are low energy dislocation structures (LEDS). This means that there will be areas of sparse dislocation population interspersed with densely packed dislocation arrays. The most common example of an LEDS is the dislocation cell which forms in materials with higher stacking fault energies (SFE). The cell is the dominant LEDS in these materials during the linear, stage II strain hardening regime. The evolution of certain cell walls into geometrically necessary boundaries (GNBs) in the form of dense dislocation walls (DDWs) and microbands (MBs) signals the onset of the non-linear stage III strain-hardening regime. These GNBs divide the grain into regions of cells of common slip called cell blocks (CBs). The cell block becomes the dominant LEDS during the large strain stage IV regime and its refinement defines the strain-hardening character. The GNBs are often macroscopically oriented near the plane of maximum shear stress (Hughes & Nix, 1989). This being the case, one can envision more possible orientations for GNBs in compression or tension as compared to torsion due to the conceptually infinite number of maximum shear stress planes which exist in pure compression or tension. In materials of lower SFE or of higher frictional stress, cross-slip becomes more difficult and the dominant LEDS during stage II becomes the Taylor lattice typified by alternating rows of edge dislocations differing by sign along the primary slip plane. Much less is known about the details of the strain hardening processes in these materials, but it has generally been observed that GNBs form and the grain is again segmented into subgrains in a manner similar to cell forming materials (Hughes, 1993).

Metals at large strains develop a preferred orientation or crystallographic texture in which certain crystallographic planes tend to orient themselves in a preferred manner in response to the applied loads or displacements. The bulk material response is a result of both texture evolution and strain-hardening processes as well as the complex interactions which naturally arise between them.

The development of deformation-induced anisotropy during large strain deformation has been demonstrated in many experiments. Comparisons between experimental observations and theoretical predictions show, however, that texture can only account for part of the observed deformation-induced anisotropy. For example, if deformation-induced anisotropy results only from the formation of texture during a rolling process, then its effect on the subsequent yield stress of specimens taken at various orientations with respect to the rolling direction could be accounted for by the modification of the stress level by the Taylor factor, M. The M factor is the ratio of the sum of the crystallographic shear strains to the macroscopic axial strain in uniaxial tension using Taylor's assumption (1938) of generalized minimum work (cf. Chin & Mammel, 1967). It has been observed, however, that this

modification can only account for part of the flow stress discrepancies. In recent work by Hansen and Jensen (1991), the observed orientation and spacing of GNBs in the form of DDWs and MBs were taken into account to accurately predict the flow stress distribution as a function of angle from the rolling axis for tensile tests conducted on cold-rolled aluminum. These GNBs are structures of immobile dislocations which provide directional resistance to motion of mobile dislocations. They altered the Petch-Hall relationship for the grain size contribution to flow stress according to

$$\sigma_{GNB} = K_h \sqrt{\frac{Gb}{D_{GNB}}} \qquad (1)$$

where D_{GNB} is the distance between geometrically necessary boundaries. Crystallographic slip is assumed to take place on planes which form an angle of 45° with respect to the tensile axis. For a given orientation, the normals to all of these planes will form a cone with its altitude direction along the tensile axis and with a half-cone angle of 45°. This model is referred to as the conical slip model. These results are very significant. As proposed by Teodosiu (1991), these results confirm that the bulk deformation behavior of a material is dependent on **both** the development of crystallographic texture and the development and evolution of dislocation substructure. The results also confirm that the stress-state dependent macroscopic orientation of the large strain GNBs plays a strong role in their evolution as well as affecting continued slip processes and strain-hardening.

Due to inherent instabilities in tension, finite strain experiments have been largely confined to uniaxial and biaxial compression as well torsion tests. Traditionally, torsion tests comprise the majority of experiments due to frictional complexities which arise at the test machine - specimen interface during a compression test. Torsion tests have been conducted on both solid circular bars and very short thin-walled tubes. An assessment of path history dependence can be made by conducting tests involving sequences of compression (or tension) and torsion. Due to experimental complexities, however, few experiments of this type have been reported.

One of the most consistently observed experimental phenomena is the softening behavior of torsion relative to compression in terms of effective stress levels at comparable equivalent plastic strain levels. This effect has been attributed to differences in crystallographic texture and, to a lesser extent, heightened strain-hardening in compression over torsion due to more slip activity in compression (Jonas et al., 1982). In light of the earlier discussion concerning the profusion of dislocation substructures in compression, the latter explanation seems more plausible, especially within the moderate strain regime. As shown by Miller & McDowell (1995), polycrystal plasticity model predictions using the Taylor model for intergranular constraint underestimate torsional softening for 304L stainless steel by roughly a factor of two, indicating that crystallographic texture alone is an inadequate descriptor of anisotropy (at least in the context of state-of-the-art models). Such results are common among structural alloys.

During free-end torsion, an axial strain develops as a manifestation of the evolution of deformation-induced anisotropy. Axial stress is induced during fixed-end tests. Monitoring and correlation of such "secondary" effects is a relevant aspect of the performance of large

strain theories.

Results from large strain shear experiments of ductile metals have been used extensively to formulate finite strain deformation models. Typically, current theories attempt to model widely observed phenomena of the large strain shear experiment on thin-walled tubular specimens; (a) lower effective stress levels based on J_2 at the same effective plastic strain compared to tension or compression tests (c.f. Bammann, 1990; Davis, 1937; Prager, 1945; Shrivastava et al., 1982), and (b) secondary, induced axial strains (free-end experiments) or axial stresses (fixed-end experiments) (Bammann, 1990; Swift, 1947, Poynting, 1909). In addition to these experimentally observable phenomena, (c) insistence of monotonicity of shear and normal stresses during torsion simulations up to physically implausible shear strain levels has been used to validate model hypotheses.

The plastic spin has been used to model behaviors (a)-(c) elucidated above. It was invoked by Dafalias (1983, 1984a, 1984b, 1985, 1987), Lee et.al.(1984), and others as a means to modify the Jaumann rate of tensorial variables to avoid oscillatory response in simple shear with kinematic hardening. The plastic spin has also been used to match axial stress developed in axially constrained tubes subjected to finite shearing (cf. Reed & Atluri, 1984), axial strain developed in free-end finite shearing tests (Bammann and Aifantis, 1987; Im and Atluri, 1987; Zbib, 1992), as well as differences between uniaxial compression or tension and torsion experiments (Bammann and Aifantis, 1987, Im and Atluri, 1987,). Unfortunately, limitations on the applicability of forms of W^p introduced over the last decade have not been clearly understood nor elucidated. Moreover, when used in the context of J_2 incompressible plasticity theory, the plastic spin required to reproduce deformation induced anisotropy effects and second order behaviors is excessive.

The objective of the modelling effort was to develop a phenomenological plasticity framework which addresses the development of anisotropy, placing the role of relative textural anisotropy and plastic spin in its proper perspective among other potential contributions to anisotropic workhardening such as formation of dislocation microbands and microstructural transformations. Within the context of incompressible plasticity, the role and interpretation of the third invariant of overstress, J_3^*, is a primary feature of this modelling effort.

A simple macroscale framework has been developed in the doctoral work of Miller (1993) within the framework of rate-independent, incompressible plasticity which incorporates the third invariant of overstress, $J_3^* = 1/3 \, tr \, (s-\alpha)^3$. The framework permits dependence on J_2 and the third invariant, $J_3 = 1/3 \, tr \, s^3$, of deviatoric stress. If kinematic hardening is employed, the second, $J_2^* = 1/2 \, tr \, s^2$, and third, J_3^*, invariant of overstress, $\Sigma = s-\alpha$ are permitted. Within the present model, J_3^* appears explicitly in the yield function and in the evolution equations of the hardening variables α and R as a means of delineating stress states effects on both initial yielding and work hardening. For example, in a free-end torsion test, $J_3^* = 0$, while for a uniaxial tension test, $J_3^* = \Sigma_{11}^3/4$, and for a uniaxial compression test, $J_3^* = -\Sigma_{11}^3/4$. It becomes apparent that an even power of J_3^* can be used to delineate torsion from tension and compression, and an odd power of J_3^* delineates compression from tension.

It has long been hypothesized that J_3^* reflects a change of constraint on slip as a function of stress state (Drucker, 1949). Slip occurs on planes oriented most closely to the plane of maximum shear stress. As discussed previously, there are an infinite number of

such planes during uniaxial compression or tension, and only two during a torsion test. It therefore seems reasonable to include J_3^{*2} as a means of accounting for heightened slip and subsequent accelerated hardening which occurs in tension and compression compared to torsion. Huffington (1991) proposed to modify the yield function using J_3 to capture similar features.

In light of the discussion on substructure presented in the previous section, this interpretation implies that the J_3^* level present during a particular stress state may have a direct impact on the nucleation, evolution, and orientation of dislocation substructures such as microbands, dense dislocation walls and other deformation substructures such as twin planes which can influence such processes as phase transformations. It is not, however, intended for use in representation of textural anisotropy.

A yield function of the form

$$f(J_2^*, J_3^*) = 3J_2^* \Psi(J_2^*, J_3^*) - R^2 \tag{2}$$

was introduced where

$$\Psi = 1 - 27\Phi\kappa J_3^{*2} / 16 J_2^{*3} - 3\sqrt{3}(1-\Phi)\kappa J_3^* / 8 J_2^{*3/2} \tag{3}$$

with the limits $0 < \kappa < 1$ and $1/2 < \Phi < 1$. The form with $\Phi = 1$ has been employed (cf. Drucker, 1949) in the context of pure isotropic hardening to correlate tests on thin walled tubes under axial tension and internal pressure subjected to varying ratios of axial stress to circumferential stress. For $\Phi = 1$, tension and compression are equivalent on the basis of J_2^*, while for $\Phi = 1/2$, compression and shear are equivalent but tension has a higher effective stress based on J_2^*. The yield function reduces to that of von Mises for $\kappa = 0$, and lies in-between the von Mises and Tresca criteria for nonzero κ with $\Phi = 1$. Experimental observations (cf. Shrivastava et al., 1982; Miller & McDowell, 1992) often reveal that κ is zero initially, and develops with cumulative plastic strain, if at all. In general, it is necessary to change the direction of the loading path in the deviatoric stress plane at several values of finite prestrain to assign values of κ and Φ necessary to model abrupt (nearly instantaneous) changes in flow stress based on J_2^*. We assume the following evolution equation for κ:

$$\dot{\kappa} = C_\kappa(\bar{\kappa} - \kappa)\dot{p} \tag{4}$$

The normality flow rule is given by

$$D^P = \frac{1}{H}\langle \overset{\circ}{s}:n \rangle n \tag{5}$$

The Macaulay brackets are defined as $\langle g \rangle = g$ for $g > 0$ and $\langle g \rangle = 0$ for $g \leq 0$. The unit normal vector n is given by

$$\mathbf{n} = \frac{\partial f/\partial \boldsymbol{\sigma}}{\|\partial f/\partial \boldsymbol{\sigma}\|} = \left(3(\Psi + J_2^* \eta \kappa)\boldsymbol{\Sigma} - 3J_2^* \xi \kappa \, \mathbf{t}\right) / \|\partial f/\partial \boldsymbol{\sigma}\| \tag{6}$$

where $\Sigma_{ij} = s_{ij} - \alpha_{ij}$ and $t_{ij} = \Sigma_{ik}\Sigma_{kj} - 2J_2^* \delta_{ij}$. The parameters η and ξ are given by

$$\eta = 81 \, \Phi J_3^{*2} / 16 J_2^{*4} + 9\sqrt{3}(1-\Phi)J_3^* / 16 J_2^{*5/2} \tag{7}$$
$$\xi = 27 \, \Phi J_3^* / 8 J_2^{*3} + 3\sqrt{3}(1-\Phi) / 8 J_2^{*3/2}$$

A total of N multiple hardening sets are employed using an Armstrong-Frederick hardening/recovery format for the backstress, α, i.e.

$$\alpha = \sum_{i=1}^{N} \alpha_i \tag{8}$$

where the co-rotational rate of α_i is given by

$$\overset{\circ}{\alpha}_i = C_i(B_i \mathbf{n}_\alpha - G_i \alpha_i)\dot{p} \tag{9}$$

where $\mathbf{n}_\alpha = \boldsymbol{\Sigma}/\|\boldsymbol{\Sigma}\|$, G_i is a nonlinear dynamic recovery function and $\dot{p} = \|\mathbf{D}^p\|$. The evolution of the isotropic hardening variables are given by

$$\dot{R}_i = C_i H_i(\bar{R}_i - R_i)\dot{p} \tag{10}$$

Here, the function $H_i(f) = f$ for "reversible" isotropic hardening and $H_i(f) = \langle f \rangle$ for irreversible hardening (e.g. martensite formation).

We consider N hardening variable sets, representative of intermediate and long range components which account for the post-yield behavior. Saturation values for the hardening variables contain an explicit dependence on J_3^* i.e.

$$B_i = B_i^{\circ} g_i^{\alpha} \quad \text{and} \quad \bar{R}_i = \bar{R}_i^{\circ} g_i^{R} \quad i = 1,...,N \tag{11}$$

where

$$g_i^{\,j} = 1 + m_i^{\,j} 27 J_3^{*2} / 4 J_2^{*3} + n_i^{\,j} 3\sqrt{3} J_3^* / 2 J_2^{*3/2} \quad i=1,...,N \, ; \, j = \alpha, R \tag{12}$$

This representation renders the following conditions for $i = 1,...,N$ and $j = \alpha$, R: pure tension; $g_i^{\,j} = (1 + m_i^{\,j} + n_i^{\,j})$, pure compression; $g_i^{\,j} = (1 + m_i^{\,j} - n_i^{\,j})$, and pure torsion; $g_i^{\,j} = 1$. All rates are taken corotationally with the intermediate configuration. Under a small elastic strain assumption these rates are given by

$$\overset{\circ}{\alpha} = \dot{\alpha} - (W - W^P) \cdot \alpha + \alpha \cdot (W - W^P) \tag{13}$$

An expression similar to that derived by Dafalias (1984, 1985) for the component of plastic spin associated with each backstress is written as

$$W_i^P = \rho_i^D (\alpha_i \cdot D^P - D^P \cdot \alpha_i) \tag{14}$$

where

$$\rho_i^D = \zeta_i e^{C_i p} \tag{15}$$

The total plastic spin is given by

$$W^P = \sum_{i=1}^{N} W_i^P \tag{16}$$

The plastic spin is the only feature of the present framework which may reflect texturing processes, albeit indirectly. The diminished plastic role of plastic spin in this framework relative to many contemporary models based on J_2 plasticity is in accordance with the physical processes of formation of low energy dislocation structures (LEDS), subdivision of grains and development of microtexture gradients within individual grains, as well as the physically observed retardation of texture development relative to the polycrystal plasticity calculations which employ the Taylor constraint assumption of the same deformation gradient in each grain (cf. Ceccaldi et al., 1994).

Experimental compression and torsion data were correlated using the above framework (cf. Miller, 1993; Miller & McDowell, 1995), apart from the short range transients which dominated stress-strain behavior just after a change of loading path direction. These short range transients where subsequently addressed by Miller & McDowell (1995, submitted to the International Journal of Plasticity) by introduction of noncoaxiality effects in the coefficients C_i of the internal variable evolution laws.

An important consideration in model development at any scale is the determination of material constants. It should be emphasized that continuum slip polycrystal plasticity models introduce an enormous number of degrees of freedom (slip system variables for each grain) with a reasonably small number of constants (e.g. 5-7) for intragranular hardening and intergranular constraint. In contrast, macroscale models introduce a small number of variables to reflect the same physics; accordingly, the evolution laws are more complex and the number of required constants increase to the order of 10-20. As long as the constants can be identified in clusters which correspond to certain physical phenomena or experiments, this is no particular problem, particularly in view of the computational efficiency gained by the low order description of such models. The recent paper of Miller & McDowell (1995) submitted to the International Journal of Plasticity outlines the procedure for determination of material constants in the above framework. Briefly, the procedure is as follows:

1. Since $J_3^* = 0$ for pure torsion, $g_i^j = 1$. The yield parameter, $\Psi = 1$, so the yield function reduces to that of von Mises. The saturation values B_i° and $\bar{R}_i^\circ$, the initial yield strength, R_o, and the rate constants C_i^* are fit to pure torsion data. The B_i° and the plastic spin parameters ζ_i are fit to axial extension data during unconstrained simple shear. Since kinematic hardening is directly linked to the stored elastic energy associated with dislocations, it is necessary that the short range kinematic hardening saturate relatively rapidly (i.e. 10-20% strain), while the long range component comprise no greater than 5-10% of the work-hardening rate, placing some constraints on the ratios $B_i^\circ / \bar{R}_i^\circ$ and the short range coefficient C_1.

2. By employing multiple hardening sets, the model has the ability to account for hardening processes which occur on multiple scales or "ranges." The first hardening set has a relatively large rate constant and low saturation levels. This set corresponds to rapidly evolving "short range" processes which reflect slip system interaction phenomena. For very large rate constants, the evolution is often so rapid that the effect of the short range component is indistinguishable from that of the yield surface. The second set is a "long range" component used to reflect slowly evolving, deformation-induced anisotropy such as the development of crystallographic texture. The use of multiple components, α_i, has precedence in infinitesimal (Chaboche, 1987, 1989) as well as finite strain plasticity. The plastic spin formulation (Eqns. (14)-(16)) presupposes that the kinematic hardening variable, α, and the rate of inelastic deformation, $\mathbf{D}^P$, are adequate descriptors of the deformation-induced anisotropy associated with texture evolution. In the present model, assuming two sets of hardening variables, it is the long range component, α_2, which is linked to effects at this length scale; hence, $\zeta_1 = 0$.

3. The compression data are then correlated by choosing values for the m_i^j and q_i^j as well as the yield function parameters Φ, C_κ, and $\bar{\kappa}$. If tension and compression are considered as equivalent, $n_i^j = 0$ and $\Phi = 1$. During compression $J_3^{*2}/J_2^{*3} = J_3^{*2}/J_2^{*3}\big|_{max} = 4/27$; hence, $g_i^j = 1 + m_i^j$ and $\Psi = 1 - \kappa/4$. The constant $C_\kappa = C_1\big|_{compression}$ and $\bar{\kappa} = 4/9$ is the maximum value of κ possible while still maintaining convexity.

As introduced by Miller & McDowell (1995, submitted to International Journal of Plasticity), additional constants relate to terms which are introduced to model the short range transients of the equivalent stress-strain response of compression-followed-by-torsion tests. These additional constants can only be determined from sequence experiments.

The axial extension of the torsion specimens appeared to be essentially independent of compressive prestrain for 304L stainless steel, indicating that hardening during compression is primarily isotropic; any appreciable amount of directional hardening along the compression axis would result in an exaggerated amount of extension upon reloading in torsion. The axial extension was similar to pure torsion, so some degree of kinematic hardening must be taking place during torsion. Assigning negative values to the m_i^α assumes that the saturation level of kinematic hardening is higher in torsion than in compression, permitting correlation of second order axial effects in simple shear. Physically, the justification of negative m_i^α values rests on the argument that compression exhibits more intense slip activity and relatively more directionally uniform dislocation structures than does

shear; hence, hardening is assumed to be more directional in torsion. This has been verified recently (Horstemeyer, 1995) using continuum double slip crystal plasticity calculations which assume slip system kinematic hardening laws of a form analogous to Eqn. (13) and intergranular constraint dependent upon the magnitude of kinematic hardening. Specifically, these calculations clearly reveal a higher degree of kinematic hardening in torsion than in compression due to the relatively lower number of systems activated in torsion on average. Similarly, these calculations reveal that the form of the plastic spin relation in Eqn. (14) offers a reasonably accurate description of the polycrystal averaged plastic spin evolution in shear, provided the magnitude of such spin is of physically appropriate magnitude.

Figures 6-7 show the excellent correlation achieved with the model for both the effective stress versus plastic strain and axial extension for 304L stainless steel (Miller & McDowell, 1995).

As discussed in the thesis of Marin (1993) and related papers (Marin & McDowell, 1995), the preceding dependence upon J_3^* can be readily embedded within the flow rule and evolution equations of internal variables of standard internal variable viscoplasticity theory. This represents a topic of continued research (Horstemeyer, 1995), particularly in terms of the influence on localization and failure, temperature- and rate-history dependence, etc.

In summary, significant advances in modelling have been achieved in this program, based on experiments and macroscale/microscale modelling. The most important concepts developed include:

- slip constraint (J_3^*) effect in both yield surface and internal state variable evolution equations
- differential hardening in compression and shear which better represents physics of hardening than does high plastic spin values adopted in previous J_2 plasticity studies
- modelling of both short and long range transients for complex loading histories involving a change of stress state

In the next section, we present some of our microscale modelling activities during the past year which serve to clarify the basis for the introduction of dislocation substructure and grain sub-division effects via J_3^* at the macroscale.

Microscale:

In the previous section, we motivated the development of the macroscale internal state variable model by virtue of the need to address effects of substructure on anisotropy of flow stress, in addition to texture. In this section, we show that the stress-strain behavior during sequences of loading predicted by a state-of-the-art polycrystal plasticity model which considers only texture as a source of anisotropy is inaccurate. Moreover, the rate of predicted texture development is too rapid. While the macroscale model has addressed these effects, albeit somewhat indirectly by comparison, these results point to the need to implement similar modifications of crystal plasticity theory to achieve a physically viable solution. While the results of the preceding sections have appeared or have been submitted to journals for publication, the following material has not yet culminated in publication; accordingly, we briefly present salient results.
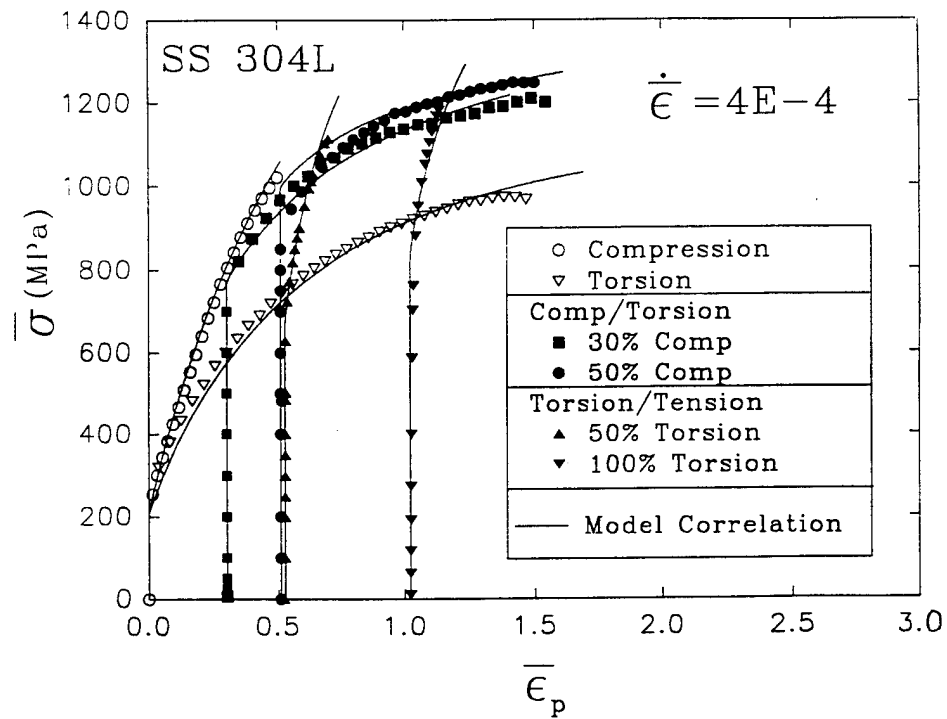
Figure 6   Macroscale model correlation of effective stress versus plastic strain for 304L stainless steel.
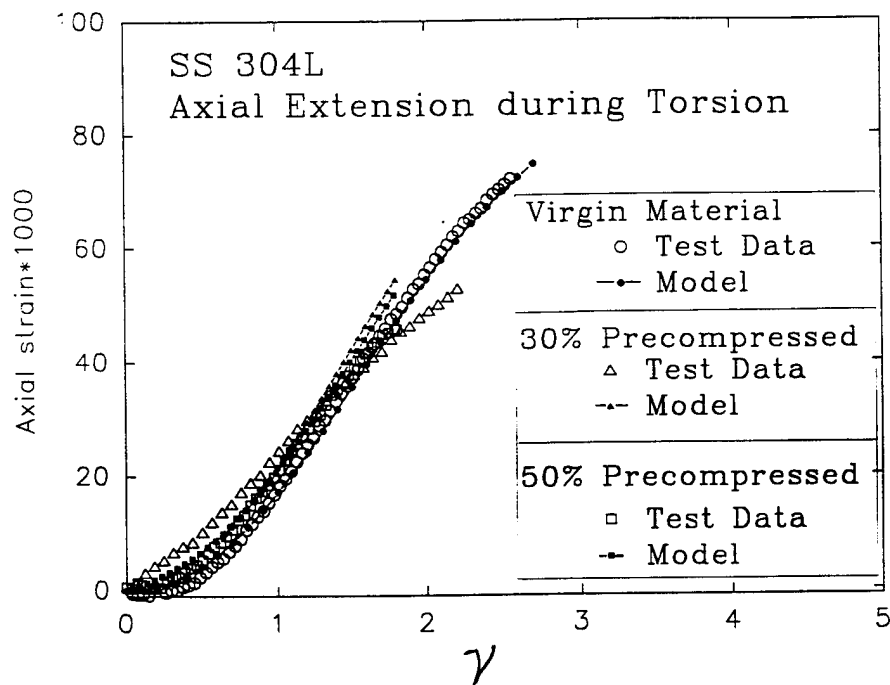

Figure 7   Macroscale model correlation of axial extension behavior during finite shear for 304L stainless steel.

The LApp (Los Alamos polycrystal plasticity) code was obtained from Fred Kocks at LANL and was employed to predict compression and sequences of compression followed by shear for OFHC Cu, once the slip system hardening variables and intergranular constraints were selected to fit pure torsion data. LApp represents a state-of-the-art simulation tool for polycrystal deformation analysis. Several hundred grains with initially random orientation may be selected to represent a material point in this code. LApp employs the assumption of a Voce law for strain hardening on each slip system, with the choice of either self-hardening (same hardening on all slip systems) or latent hardening (40% higher on secondary slip systems). Furthermore, the user can select either full constraints (Taylor assumption) or relaxed constraints; the latter is regarded as somewhat more appropriate as the grains deformation at large strains. Elasticity is neglected in this code.

In the following figures, the flow stress reported is the uniaxial equivalent J_2 flow stress, while the plastic strain is the uniaxial equivalent Mises plastic strain. Figure 8 shows the correlation obtained for pure torsion of OFHC Cu using the LApp code with self hardening (LApp prediction) and with latent hardening (LApp, Latent Hardening). Figure 9 compares the prediction of the LApp code for pure compression with and without latent hardening, as well as with relaxed constraints. The latent hardening with the Taylor assumption appears to predict the compression response rather well. At this point, it is tempting to conclude that the polycrystal plasticity theory accurately reflects the physics of large strain deformation since torsional softening is predicted.
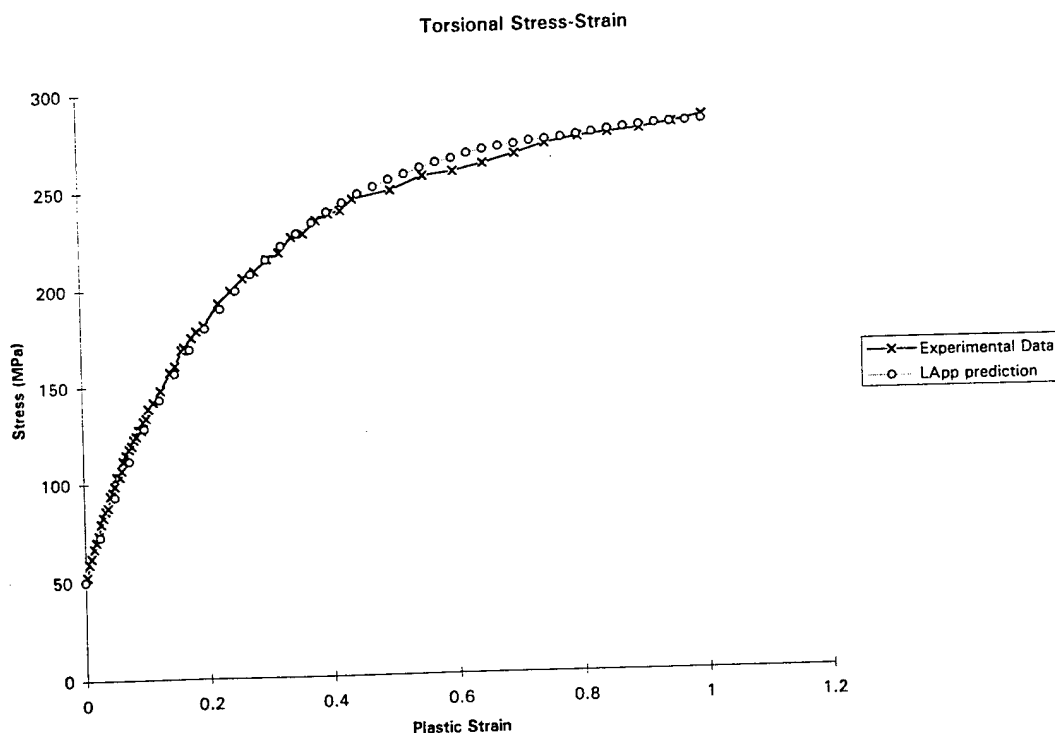
Torsional Stress-Strain

Figure 8   Correlation of LApp code calculations (used to determine material constants) for pure torsion of OFHC Cu.
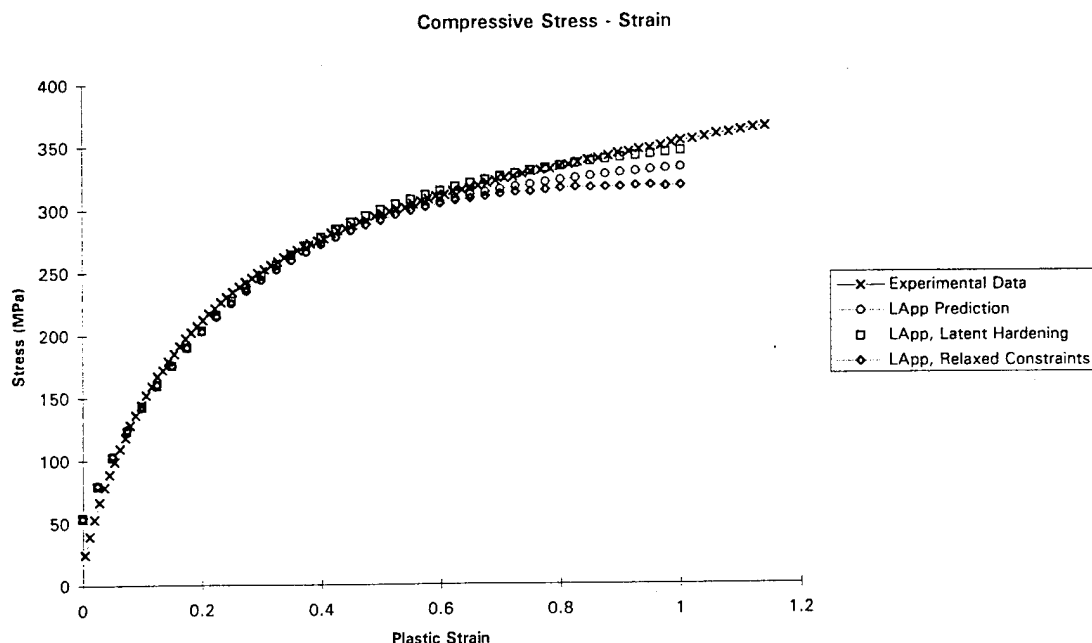
Compressive Stress - Strain

Figure 9   Prediction of LApp code calculations for pure compression of OFHC Cu with and without latent hardening and relaxed constraints.

However, consideration of sequence experiments uncovers some inconsistency with physical phenomena, analogous to the role of nonproportional loading paths in sorting out physically viable hardening laws at small strains (cf. McDowell, 1985). Figure 10 compares the predictions of the LApp code with various options with experimental results for a sequence of compression followed by torsion. Clearly, all of the LApp options result in very little difference in predicted response. Interestingly, the predicted flow stress is well below (approximately only 30%-40% of the difference between torsion and compression) the effective flow stress observed in subsequent torsion. Furthermore, the rate of strainhardening decreases (well below that of pure torsion) and the flow stress merges into that of virgin torsion response after subsequent effective plastic strain on the order of the prestrain, quite contrary to the experiment. Likewise the observed hardening in tension following torsional prestrain is underpredicted by the LApp code, as seen in Figure 11.

One of the dominant characteristics of the LApp code is its prediction of rapid evolution of texture compared to experimental measurements. Figures 12-13 compare pole figures generated from LApp using the graphics package in popLA with pole figures obtained experimentally, presented in the same format. In this case, data are presented from the longitudinal-radial planes exposed by radially sectioning the specimens. This perspective differs from that reported in most pole figures for these stress states obtained from solid specimens; accordingly, the poles appear in different locations. Note that information outside of the ring approximately 70° from the center are omitted in the experimental pole
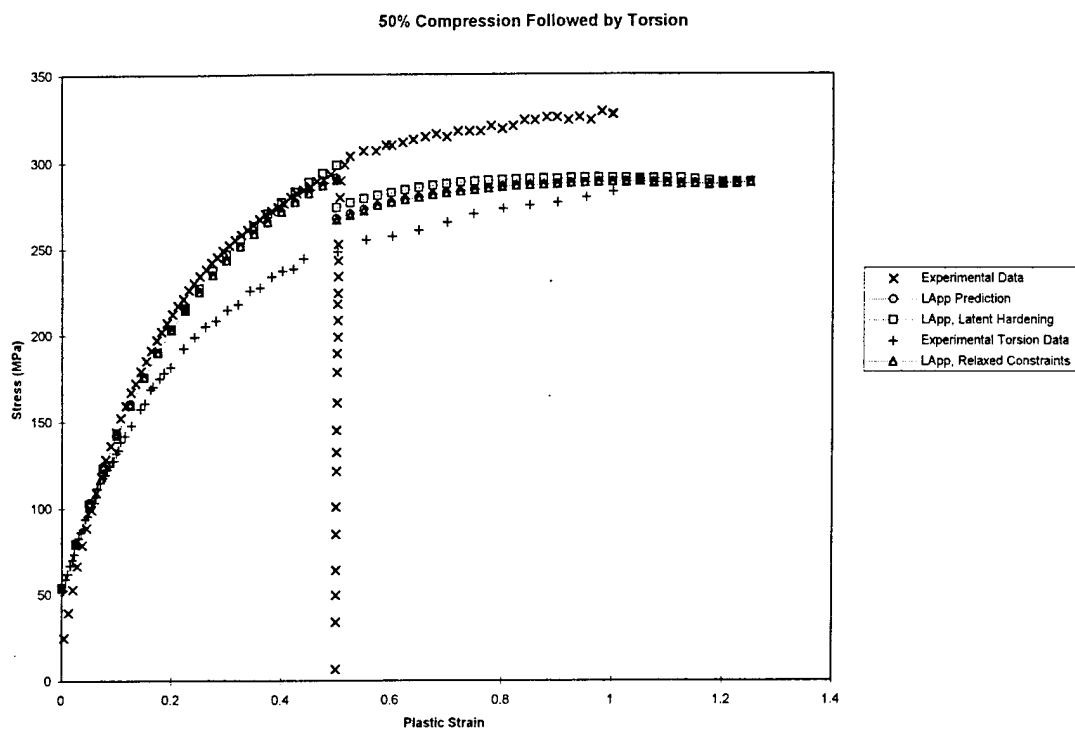
Figure 10   Comparison of predictions of LApp code with experiments for a sequence of compression followed by torsion.
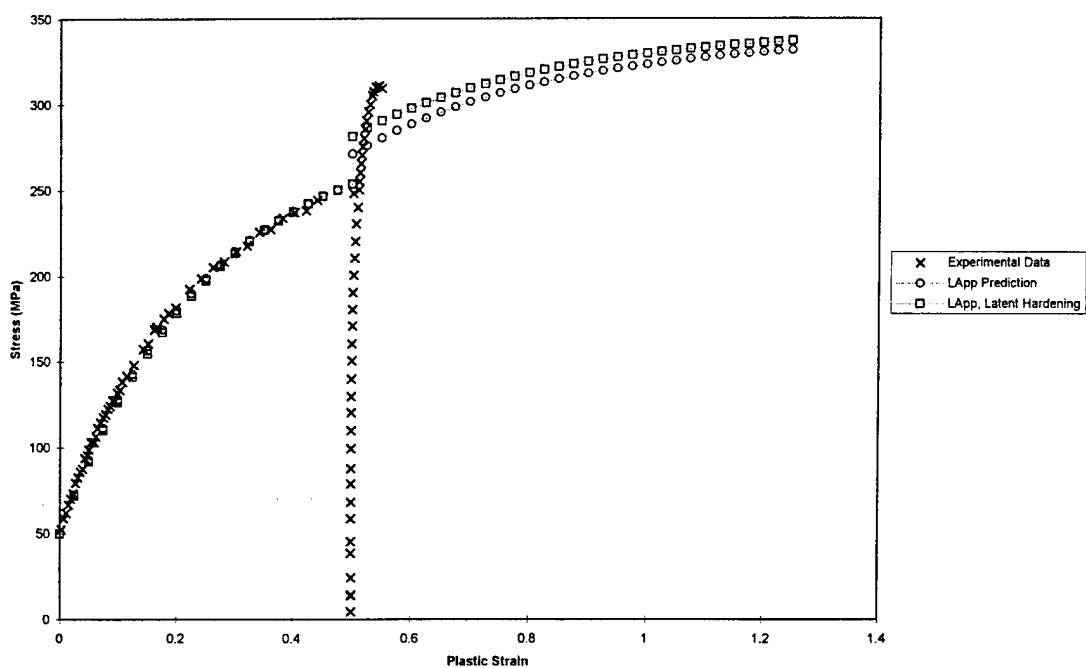

Figure 11   Comparison of predictions of LApp code with experiments for a sequence of torsion followed by tension.

figures due to uncertainty of the measurements at these diffraction angles. The peaks of texture are in the same location and the pole figures exhibit the same symmetries. Although it is not possible to compare the intensities directly, by comparing the relative intensities of peak regions to background levels (valleys) it is seen that the predicted textures are sharper than those experimentally measured, with relative intensities of peaks roughly an order of magnitude higher. This likely accounts for the prediction of the subsequent torsion merging into the pure torsion curve in Figure 10, since the texture will evolve rapidly and so the polycrystal ensemble will appear to correspond to that of pure torsion at 100% effective plastic strain, without lasting memory of the compressive prestrain.
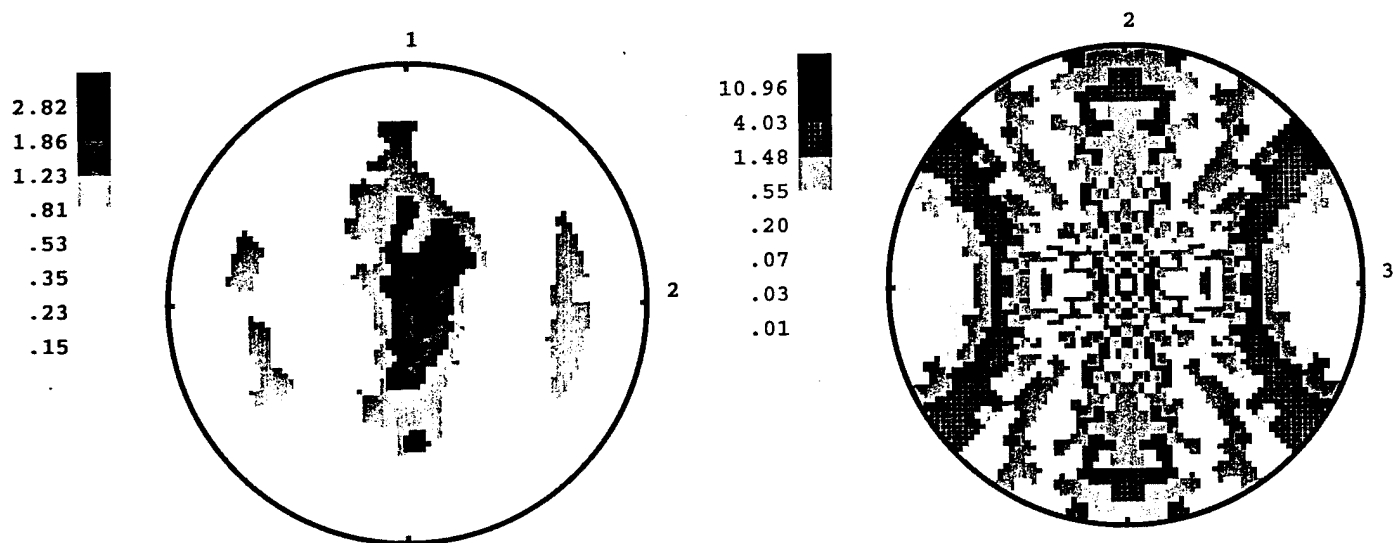

Figure 12   Comparison of experimentally measured 111 pole figure from popLA (left) with that predicted by the LApp code with Taylor constraint (right) for 50% plastic strain in compression.
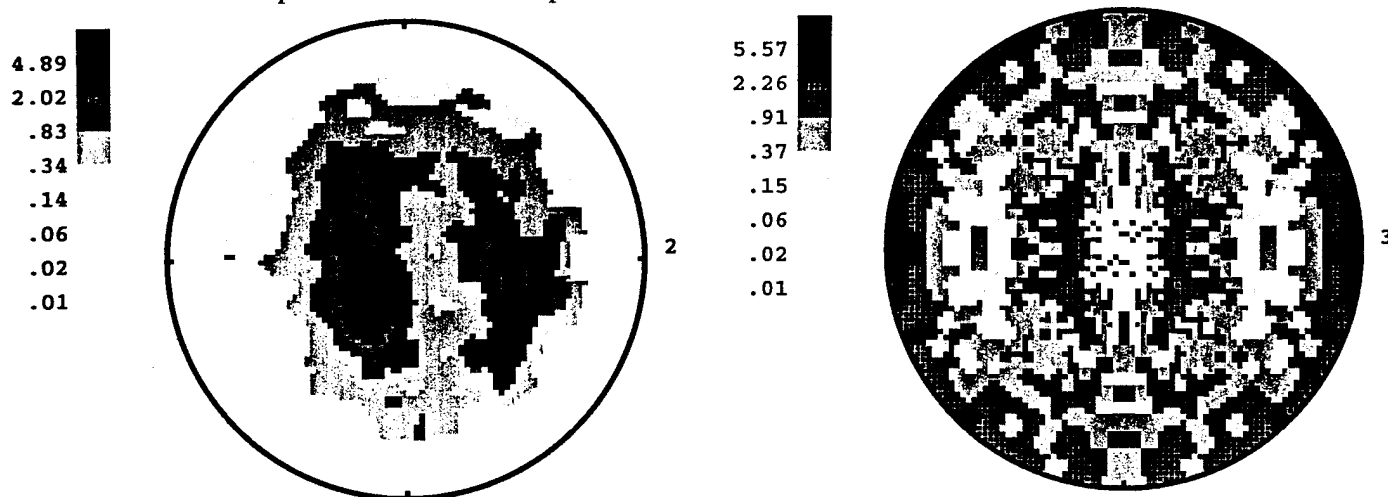

Figure 13   Comparison of experimentally measured 111 pole figure from popLA (left) with that predicted by the LApp code with Taylor constraint (right) for 50% effective plastic strain in torsion.

Figure 14 shows the Taylor factors computed with the LApp code for compression, torsion, and sequences of stress state. Clearly, the torsional softening is a result of Taylor factors which start at different levels and evolve in opposite directions, as is well-established. Since each grain is assumed to be of uniform orientation and size, the jump of Taylor factor during a path change varies only to a slight degree with cumulative strain. The evolution of the Taylor factor after the path change occurs at a rate comparable to the rate of change of the Taylor factor for the monotonic loading paths at the same level of effective plastic strain.
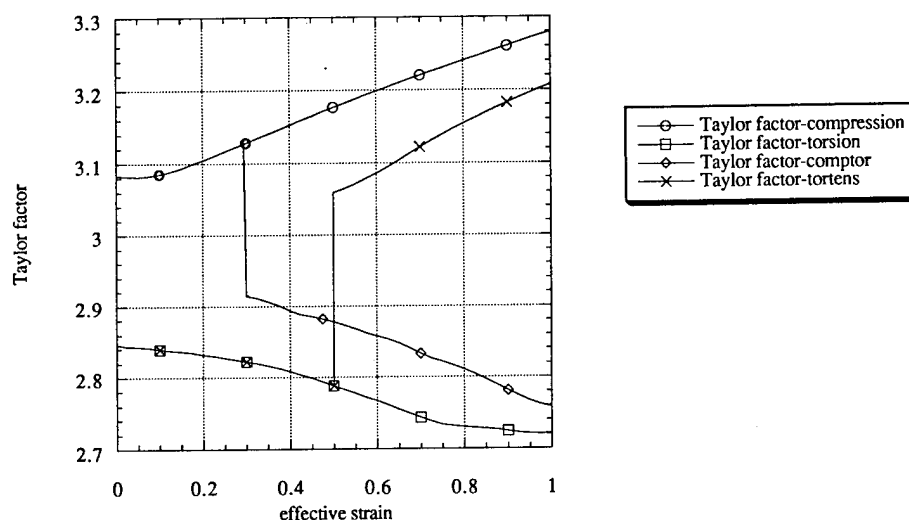

Figure 14   Evolution of Taylor factors for several different straining paths determined from the LApp code with Taylor constraint. strain in torsion.

This overprediction of texture and lack of a repository for path dependent differences in slip between compression and shear are two features of state-of-the-art crystal plasticity models which cannot be fully addressed by adjustments of the slip system hardening laws and intergranular constraints. Rather, the theory requires additional features at the sub-grain scale which relate to differences of grain-subdivision between compression and torsion (e.g. non-Schmid effects). Work along these lines is taking place at RIS0 in Europe, and is one of the topics being investigated in the AASERT award which parallels this program.

An interesting set of experiments concerned the change of the elastic modulus ($\lambda +$ 2μ), where λ and μ are the Lamé constants, obtained by measurement of the longitudinal wavespeed in original and deformed specimens. Figure 15 shows the reduction of the elastic modulus as a function of plastic strain for pure compression, both in the direction of compression as well as the direction transverse (orthogonal) to compression. Also shown is the increase of the elastic moduli following compression orthogonal to the original compression direction, obtained by re-machining a cylindrical specimen following the first compression event. The predictions of planar double slip polycrystal plasticity are also shown. Clearly, the model predictions are qualitatively in agreement, but the experimental disparity of transverse and longitudinal moduli and the overall magnitude of the effect are

not well-predicted. In this case, the overprediction of the modulus reduction is due to the unrealistically high rate of texture evolution (and elastic anisotropy) predicted by the Taylor model. Consequently, the prediction of coupled elasto-plastic wave propagation during dynamic plasticity would be affected, in addition to the degree of elastic and plastic anisotropy.

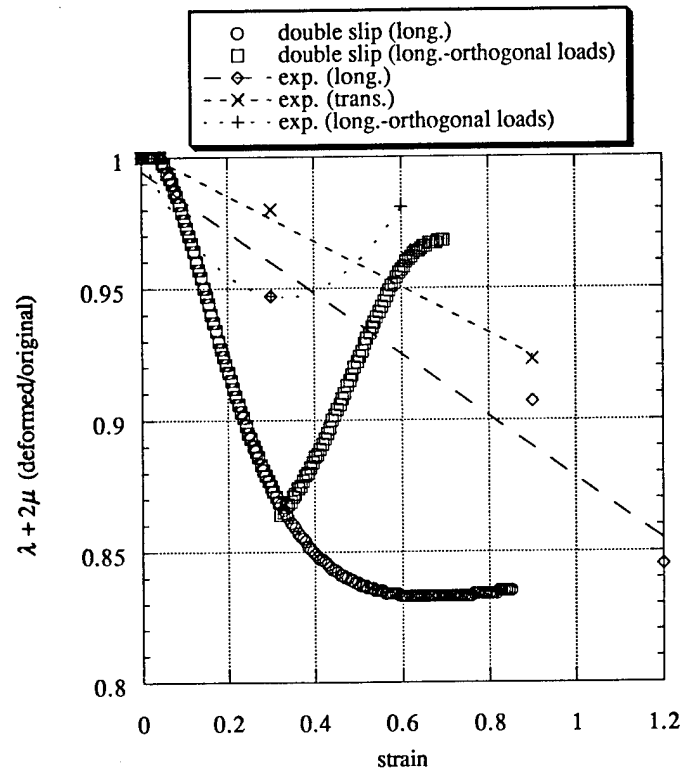Figure 15   Evolution of the elastic modulus ($\lambda + 2\mu$) in the direction of compression and orthogonal to this direction from longitudinal wavespeed measurements for pure compression and for a sequence of compression to 30% plastic strain, followed by compression in an orthogonal direction.

More details will be provided concerning this work in the future theses and papers of M. Horstemeyer and G. Butler.

III. Student & Faculty Involvement and Interactions

Graduate Degrees Conferred:

1. Miller, M.P., "Improved Constitutive Relations for Finite Strain Inelastic Deformation," Ph.D. Thesis, G.W. Woodruff School of Mechanical Engineering, Georgia Tech, defended June 1993. Dr. Miller presently holds a position as Assistant Professor in the Sibley School of Mechanical Engineering at Cornell University.
2. Marin, E.P., "A Critical Study of Finite Strain Porous Inelasticity," Ph.D. Thesis, G.W. Woodruff School of Mechanical Engineering, Georgia Tech, defended December 1993; currently post doctoral researcher at Cornell University in Paul Dawson's group.
3. Graham, S., Jr., "The Stress State Dependence of Finite Inelastic Deformation Behavior of F.C.C. Polycrystalline Materials," M.S. Thesis, March 1995.
4. Lustig, S.K., "Microstructural Analysis of Finite Deformation of FCC Polycrystals," M.S. Thesis, March 1995.

Other Graduate Students Involved:

Mark Horstemeyer, a Ph.D. student sponsored by Sandia-Livermore who started in Fall 1993, is extending Marin's doctoral work to include textural/substructural anisotropy effects in a rate- and temperature-dependent internal state variable model framework to be implemented in ABAQUS, DYNA and PRONTO. He is also working to incorporate results of 2-D crystal plasticity calculations concerning orientation distribution functions and texture into macroscale internal state variable theory suitable for large scale structural calculations under dynamic conditions.

In an associated AASERT award, Mr. George Butler is pursuing texture measurement, micromechanical modelling of texture and substructure using crystal plasticity concepts, and the development of improved hardening laws and linkages between micro- and macro-internal state variable models.

Undergraduate Student Participation:

1. J.K. Jacobus, previously a senior Mechanical Engineering student, participated in the experimental program for one year, assisting in development of optical and capacitance devices to measure axial extension during finite free-end torsion. Mr. Jacobus is presently pursuing a graduate degree in Mechanical Engineering at the University of Illinois at Urbana-Champaign.
2. P. Buzyna, a Mechanical Engineering undergraduate student, has assisted with preparation of specimens for mechanical testing and texture measurement.

Faculty Involvement:

The following faculty members have been supported by the project:

1. D.L. McDowell, Professor of ME, Project PI/PD. In charge of experimental program, constitutive equation development, overall program at Georgia Tech and coordination with Sandia National Laboratories in Livermore, CA.
2. S.R. Stock, Associate Professor of MSE. Responsible for overseeing texture measurements on compression, torsion and sequential test specimens.
3. Y.K. Lee, Assistant Professor of ME. Responsible for least squares finite element implementation as alternative to displacement-based FE schemes for finite deformation (during first year of grant).

It is anticipated that several significant journal articles will emerge from the collaborations with Dr. Stock and the AASERT student, George Butler, regarding quantification of texture for the mechanical experiments performed in this program. In conjunction with Horstemeyer's work, Butler will further develop linkages between microscale and macroscale theories which better express the role of subgrain deformation processes.

Interaction with Sandia National Laboratories, Livermore, CA:

Participants at Sandia-Livermore, by area of technical interest, include:

D.J. Bammann - Macroscale modeling
M.L. Chiesa - Finite element implementation
W. Kawahara - Monotonic and sequential compression tests
D. Hughes - Microstructure characterization & interpretation
M. Horstemeyer - Micro- to macro- models; finite element implementation (expected to complete Ph.D. at Georgia Tech in August 1995)

Interaction with U.S. Army Research Laboratories:

In terms of interactions with U.S. Army Research Laboratories, Dr. McDowell visited the ARL in Aberdeen on July 12, 1993 and presented a seminar regarding this project entitled *Substructure and Porosity Considerations for Modeling Finite Strain Inelasticity of Metals.* The ARL host was Dr. Jack Huffington. Meetings were held with analysts involved in explosively formed penetrator and shape charged jet applications, along with managers of computational analysis branches. The intent was to foster ties with the ARL so that once documented, model developments can be implemented in codes of interest to the U.S. Army. The future development of damage-coupled viscoplastic finite element subroutines for use by ARL scientists and engineers is an intended long-term outcome of these interactions.

In addition, D.L. McDowell participated in the U.S. Army Symposium on Solid Mechanics, Plymouth, MA, 17-19 August, 1994 and presented the paper *Modelling Substructural and Textural Anisotropy at Finite Strain* co-authored with M.P. Miller and D.J. Bammann.

PUBLICATIONS

1. Miller, M.P. and McDowell, D.L., "Stress State Dependence of Finite Strain Inelasticity." Microstructural Characterization in Constitutive Modeling of Metals and Granular Media, ASME MD - Vol. 32, Ed. G.Z. Voyiadjis, Phoenix, AZ, April 1992, pp. 27-44.

2. McDowell, D.L., Marin, E., Lee, Y.K. and Miller, M.P., "Considerations for a 'Complete' Theory of Multiaxial Inelasticity for Ductile Metals," Proc. MECAMAT '92, Int. Seminar on Multiaxial Plasticity, Cachan, France, 1-4 September, 1992.

3. Miller, M.P., McDowell, D.L., Lee, Y.K. and Bammann, D.J., "Anisotropy and Path Dependence in Finite Deformation Shear and Sequential Compression/Shear," Proc. Asia-Pacific Symp. on Advances in Engineering Plasticity and its Application, Hong Kong Polytechnic, Hong Kong, 15-17 December, 1992.

4. Miller, M.P., McDowell, D.L., and Bammann, D.J., "Finite Strain Sequence Effects for 304L Stainless Steel," Proc. Fourth Int. Symp. on Plasticity and its Current Applications, Baltimore, July 23-24, 1993.

5. Miller, M.P., McDowell, D.L., and Bammann, D.J., "Modelling Substructural and Textural Anisotropy at Finite Strain," presented at the U.S. ARMY Symp. on Solid Mech., Plymouth, MA, Aug. 17-19, 1993.

6. McDowell, D.L., Marin, E. and Bertoncelli, C., "A Combined Kinematic-Isotropic Hardening Theory for Porous Inelasticity of Ductile Metals," International Journal of Damage Mechanics, Vol. 2, April 1993, pp. 137-161.

7. Miller, M.P. and McDowell, D.L., "Stress-State Dependent Deformation Behaviour of FCC Polycrystals," Proc. 15th Ris0 Int. Symp. on Materials Science: Numerical Predictions of Deformation Processes and the Behaviour of Real Materials, eds. S.I. Anderson et al., Roskilde, Denmark, 1994, pp. 421-426.

8. McDowell, D.L., "Multiaxial Effects in Metallic Materials," ASME AD-Vol. 43, Durability and Damage Tolerance, 1994, pp. 213-267.

9. Miller, M.P. and McDowell, D.L., "The Effect of Stress-State on the Large Strain Inelastic Deformation Behavior of 304L Stainless Steel," to appear in ASME J. Engng. Mater. Techn., 1995.

10. Marin, E.B. and McDowell, D.L., "A General Framework for Porous Viscoplasticity," submitted for presentation at NUMIFORM '95, Cornell University, June 18-21, 1995.

11. Miller, M.P. and McDowell, D.L., "Biaxial Tests of Material Subjected to Large Torsional Prestrains," presented at the ASTM Symp. on Multiaxial Fatigue and Deformation Testing Techniques, Denver, May 15, 1995 (to be reviewed for publication in an ASTM STP).

12. Miller, M.P. and McDowell, D.L., "Stress-State Sequence Effects on Large Strain Deformation Behavior of F.C.C. Polycrystals," submitted for publication to the International Journal of Plasticity, April 1995.

13. Marin, E.B. and McDowell, D.L., "Models for Compressible Elasto-Plasticity Based on Internal State Variables," submitted for publication to the International Journal of Damage Mechanics, May 1995.

14. Marin, E.B. and McDowell, D.L., "Associative Versus Non-Associative Porous Viscoplasticity Based on Internal State Variable Concepts," submitted for publication

in the Int. J. Plasticity, March 1995.

In preparation:

15. Marin, E.B. and McDowell, D.L., "A Semi-Implicit Integration Scheme for Rate-Dependent and Rate-Independent Plasticity," to be submitted for publication in the Int. J. Numer. Meth. Engng or equivalent.
16. Graham, S., Lustig, S., McDowell, D.L., Hughes, D. and Kawahara, W., "Effects of Finite Strain Loading Sequence on Structure and Behavior of FCC Polycrystals," to be submitted for publication in Acta Metal.

INTERNATIONAL VISIBILITY: WORKSHOPS

Such a comprehensive experimental program provides a very stringent test of predictive and/or correlative capabilities of existing crystal plasticity and macroscale polycrystal models for finite strain. Very few, if any, equivalent datasets are currently available in the open literature. Accordingly, at a recent NSF Workshop entitled "An Evaluation of Constitutive Models For Finite Plastic Deformation in Solids" (Baltimore, MD, July 23-24, 1993, Chairman A. Khan), *the experimental data which has emerged from this project was selected as the benchmark experimental database for an international effort in evaluation of constitutive models.* As such, mechanical test data, texture measurements, etc. will be made available to all interested participants.

D.L. McDowell, along with Co-PI S.D. Antolovich of Washington State University, received funding from the NSF to conduct two workshops in the subject mechanics and processing of advanced engineered materials. The first workshop was held in Pullman, WA Oct. 11-13, 1993. D.L. McDowell presented the following lecture:

McDowell, D.L., "Multiaxial Effects in Metallic Materials," NSF Workshop on Processing and Modelling of Advanced Engineered Materials, Washington State University, Pullman, WA, October 11-13, 1993.

The second workshop was held at Lake Lanier Islands in Georgia, October 24-26, 1994. Both workshops involved representatives of academia, government agencies and industry.

The topic of these workshops, mechanics and processing of advanced engineered materials, motivated much discussion regarding the role of length scales in mechanics modelling, the possible impact of such models on the development of processing science, and the necessity of interdisciplinary programs to provide a conceptual framework in which to address the link between processing and mechanics. Much of the technical content of the workshop revolved around issues of length scales at which certain physical processes are active, as well as effects of a collective set of different length scales and the averaging processes necessary to incorporate information relevant to such scales in macroscale constitutive relations and corresponding process models. The theme of these workshops was very much related to the topic of this ARO grant, since they addressed features at the microstructural scale which affect macroscopic response.

HONORS AND AWARDS

Honors and awards of D.L. McDowell (PI/PD) include:

1. Woodruff Fellow, Woodruff School of Mechanical Engineering, Georgia Tech, 1991-1996
2. Institute Fellow, Georgia Tech, 1994-1999
3. Medaile de'honneur, Societe Francaise de Metallurgie et de Materiaux (SF2M), 1994

Dr. McDowell was selected to serve as one of 15 members of the Defense Science Study Group (DSSG) for 1992-93 sponsored by ARPA and administered by the Institute for Defense Analyses (IDA) in Alexandria, VA. This prestigious, highly competitive two-year appointment involved study of high level technology and national security issues. The two-year program included visits to DoD contractors, military bases, and defense-related government installations. Through this program, ongoing national level advisory and analysis needs can be addressed with new generations of researchers.

Members were selected from academia and are typically in their mid-30's to mid-40's. The DSSG members for 1992-1993 included:

Peter Chen, Dept. Chemistry, Harvard Univ.
William J. Dally, Dept. Elec. Engng. and Comp. Sci., MIT
Mark E. Davis, Dept. Chem. Engng., Cal Tech
S. James Gates, Jr., Dept. Physics and Astronomy, Univ. Maryland/Howard Univ.
Nancy M. Haegel, Dept. Mater. Sci. Engng., UCLA
Thomas C. Halsey, Dept. Physics, Univ. Chicago
Robert A. Hummel, Dept. Comp. Sci., Courant Institute, New York Univ.
Kevin K. Lehmann, Frick Chem. Labs and Dept. Chem., Princeton Univ.
David L. McDowell, School of Mech. Engng., Georgia Tech
Anne B. Meyers, Dept. Chem., Univ. Rochester
Gerald A. Navratil, Dept. Applied Phys., Columbia Univ.
Robert A. Pascal, Frick Chem. Labs and Dept. Chem., Princeton Univ.
Dennis L. Polla, Dept. Elec. Engng., Univ. Minnesota
Peter W. Voorhees, Dept. Mater. Sci. Engng., Northwestern Univ.

Mentors of these participants, selected from the ranks of military and academic/industrial defense advisors, help to guide discussions and study topics. Several retired Generals participated as mentors, including Gen. A.J. Goodpaster, Gen. R.E. Dougherty, Gen. P.F. Gorman, Gen. I.C. Kidd, Gen. W.Y. Smith, G. H.D. Train, II, and Gen. L.D. Welch, who also serves as President and CEO of IDA. Gen. Smith serves as Chairman of the DSSG. Academic, government and industrial mentors include D. Alpert, R.S. Berry, R. Davis, A.H. Flax, S.E. Koonin, M. Krebs, S.S. Penner, D. Pines, R.E. Roberts and H. York. Dr. Julian Nall of IDA is the Program Director, reporting directly to Program Manager Dr. Ira D. Skurnick and Dr. Gary L. Denman of (D)ARPA.

Group members conducted independent studies/analyses of important defense technology and policy issues. Dr. McDowell co-authored the study *"An Assessment of the*

State-of-the-Art in Constitutive Modeling and Hydrocodes for Ballistic Impact and Blast Waves" with Professor P. Voorhees of Northwestern University. This report, which deals with dynamic material deformation and failure behavior, discusses the current state-of-the-art of material modelling and numerical simulation for impact damage and offers considerable insight into the practical applications of some of the concepts being developed in this current ARO-sponsored research project. The report is presently in ARPA review prior to distribution by IDA. Distribution to ARO will be forthcoming. A condensed version will be submitted to the International Journal of Impact Engineering for publication.

REFERENCES

Bammann, D.J. and Aifantis, E.C., Acta Mechanica, 69 pp. 97-117 (1987).

Bammann, D.J., Applied Mechanics Reviews, 43, 5, Part 2, E. Krempl and D.L. McDowell, eds., pp. S312-S319 (1990).

Butler, G., G.W. Woodruff School of Mechanical Engineering, personal communication, 1995.

Ceccaldi, D., Yala, F., Baudin, T., Penelle, R., Royer, F. and Arminjon, M., Deformation Textures and Plastic Anisotropy of Steels Using the Taylor and Nonhomogeneous Models, Int. J. Plasticity, Vol. 10, No 6, 1994, pp. 643-661.

Chaboche, J.L., International Journal of Plasticity, 5, No. 3, pp. 247 (1989).

Chaboche, J.L. 1989. Constitutive equations for cyclic plasticity and cyclic viscoplasticity. Int. J. Plasticity 5 (3): 247.

Chin, G.Y., and Mammel, W.L., 1967, Trans. of Met. Soc. AIME, 239, pp. 1400-1405.

Cullity, B.D., Elements of X-ray Diffraction, Second Edition, Addison-Wesley (1978).

Dafalias, Y.F., ASME Journal of Applied Mechanics, 50, pp. 561-565 (1983).

Dafalias, Y.F., Mechanics of Materials, 3, pp. 223-233 (1984a).

Dafalias, Y.F., Constitutive Equations: Macro and Computational Aspects, K.J. William, ed., ASME, New York, NY, pp. 25-40 (1984b).

Dafalias, Y.F., ASME Journal of Applied Mechanics, 107, pp. 865-871 (1985).

Dafalias, Y.F., Acta Mechanica, 69, pp. 119-138 (1987).

Dafalias, Y.F. and Aifantis, E.C., Acta Mechanica, 82, p. 31 (1990).

Davis, E., Journal of Applied Physics, 8, pp. 213-217 (1937).

Drucker, D.C., ASME Journal of Applied Mechanics, 16, pp. 349-357 (1949).

Graham, S., Jr., "The Stress State Dependence of Finite Inelastic Deformation Behavior of F.C.C. Polycrystalline Materials," M.S. Thesis, March 1995.

Hansen, N. and Jensen, D.J., Flow stress anisotropy caused by geometrically necessary boundaries. Acta Met., in press, submitted 1991.

Hansen, N., and Kuhlmann-Wilsdorf, D., 1986, Mater. Sci. Eng., 8, pp 141-161.

Hecker, S.S. and Stout, M.G., Deformation, Processing, and Structure, G. Krauss, ed, American Society for Metals, Metals Park, Ohio, pp 1-46 (1984).

Horstemeyer, M.F., G.W. Woodruff School of Mechanical Engineering, personal communication, 1995.

Huffington, N.J., A Reexamination of the Plastic Flow Criterion for Copper, Proc. 12th Army Symposium on Solid Mechanics, Ed. S.C. Chou, Plymouth, MA, pp. 509-520 (1991).

Hughes, D.A. and Hansen, N., Microstructural evolution in nickel during rolling from intermediate to large strains. Submitted to Metall. Trans. (1993).

Hughes, D.A., Acta Metall. et Mater. 41, pp. 1421-1430 (1993).

Hughes, D.A. and Nix, W.D., Materials Science and Engineering, A122, pp. 153-172 (1989)

Hughes, D.A. and Hansen, N., Materials Science and Technology, 7, pp. 544-553 (1991).

Im, S. and Atluri, S.N., International Journal of Plasticity, 3, pp. 163-191 (1987).

Kuhlmann-Wilsdorf, D., Trans. Metall. Soc. AIME, 224, pp. 1047-1061 (1962).

Kuhlmann-Wilsdorf, D. and Comins, N.R., Mater. Sci. Eng., 60, pp. 7-24 (1983).

Lee, E.H., Mallett, R.L. and Wertheimer, T.B.,ASME Journal of Applied Mechanics, Vol. 50, pp. 554-560 (1984).

Lustig, S.K., "Microstructural Analysis of Finite Deformation of FCC Polycrystals," M.S. Thesis, March 1995.

Marin, E.P., "A Critical Study of Finite Strain Porous Inelasticity," Ph.D. Thesis, G.W. Woodruff School of Mechanical Engineering, Georgia Tech, defended December 1993.

Marin, E.B. and McDowell, D.L., "Models for Compressible Elasto-Plasticity Based on Internal State Variables," submitted for publication to the International Journal of Damage Mechanics, May 1995.

Marin, E.B. and McDowell, D.L., "Associative Versus Non-Associative Porous Viscoplasticity Based on Internal State Variable Concepts," submitted for publication in the Int. J. Plasticity, March 1995.

McDowell, D.L., 1985, "An Experimental Study of the Structure of Constitutive Equations for Nonproportional Cyclic Plasticity," ASME Journal of Engineering Materials and Technology, Vol. 107, pp. 307-315.

McDowell, D.L., Miller, M.P., and Bammann, D.J., MECAMAT '91, Proceedings of the International Seminar on Large Plastic Deformations, Fountainebleau, France (1991).

Miller, M.P. and McDowell, D.L., Microstructural Characterization in Constitutive Modeling of Metals and Granular Media, ASME MD 32, G.P. Voyiadjis, Editor, pp. 27-44. (1992).

Miller, M.P., "Improved Constitutive Relations for Finite Strain Inelastic Deformation," Ph.D. Thesis, G.W. Woodruff School of Mechanical Engineering, Georgia Tech, defended June 1993.

Miller, M.P. and McDowell, D.L., "The Effect of Stress-State on the Large Strain Inelastic Deformation Behavior of 304L Stainless Steel," to appear in ASME J. Engng. Mater. Techn., 1995.

Miller, M.P. and McDowell, D.L., "Biaxial Tests of Material Subjected to Large Torsional Prestrains," presented at the ASTM Symp. on Multiaxial Fatigue and Deformation Testing Techniques, Denver, May 15, 1995 (to be reviewed for publication in an ASTM STP).

Miller, M.P. and McDowell, D.L., "Stress-State Sequence Effects on Large Strain Deformation Behavior of F.C.C. Polycrystals," submitted for publication to the International Journal of Plasticity, April 1995.

Poynting, J. H., Proceedings of the Royal Society of London, A82, pp. 546-558 (1909).

Prager, W., Journal of Applied Physics, 16, pp. 837-840 (1945).

Reed, K.W. and Atluri, S.N., Constitutive Equations: Macro and Computational Aspects, K.J. William, ed., ASME, New York, NY, pp. 111-129 (1984).

Shrivastava, S.C., Jonas, J.J. and Canova, G., Journal of the Mechanics and Physics of Solids, 30, No.1/2, pp. 75-90 (1982).

Swift, H.W., Engineering 163, pp. 253-257 (1947).

Taylor, G.I., 1938, J. Inst. Metals, 62, pp. 307-324.

Teodosiu, C., 1991, in Anisotropy and Localization of Plastic Deformation, J.-P. Boehler and A.S. Khan eds, pp. 179-182.

Thompson, R.B., Smith, J.F., Lee, S.S. and Johnson, G.C., "A Comparison of Ultrasonic and X-ray Determinations of Texture in Thin Cu and Al Plates," Met Trans 20A, pp. 2431-2447 (1989).

Zbib, H.M. Microstructural Characterization in Constitutive Modeling of Metals and Granular Media, ASME MD 32, G.P. Voyiadjis, Editor, pp 45-53. (1992).

APPENDIX A

DATAFILES FOR MECHANICAL TESTS AT FINITE STRAIN

This Appendix attempts to provide a self-contained summary of the data format for dissemination. It is also intended to provide a brief explanation of data reduction procedures.

I.1 Materials

The materials tested in this program were 304L stainless steel, OFHC copper, and 6061-T6 aluminum. Materials used in this experiment were annealed after final machining into test specimens except specimens containing a prestrain history. Stainless steel material was annealed in vacuo for one hour at 950°C. The chamber was back-filled with argon and the material was cooled to 500°C in 300 seconds and then cooled to ambient conditions. OFHC copper material was annealed in vacuo for one hour at 600°C and then removed from the oven to cool to ambient temperature. The 6061-T6 aluminum was annealed per the T6 standard. The material was soaked at 412°C - 440°C for two hours, furnace cooled at a maximum rate of 10°C/min to at least 260°C, and then cooled to ambient conditions. The resulting initial grain sizes for the materials were

as follows:

              304 L SS   27μm

              OFHC Cu   37μm

Mean grain size measurements of 6061-T6 Al have not been performed.

I.2 Tests

A representative set of data from tests of each material and each prestrain history (e.g. prestrain levels of 0%, 30%, 60%, etc.) is included. These representative tests of OFHC copper, 304L stainless steel, and 6061-T6 aluminum, consist of the following:

(1)   One large strain free-end torsion test for each material.

(2)   One large strain homogenous compression test.

(3)   One large strain compression test followed by re-machining and subsequent large strain torsion for each material and prestrain history.

A complete listing of experiments appear in Table 3.

Table 3. Tests for Dissemination.

304L SS		
Test Mode	Prestrain	Cumulative $\bar{\epsilon}_p$ Level (%)
Compression	0	50
Torsion	0	100
Compression/ Torsion	30% compression	100
Compression/ Torsion	50% compression	100
Torsion/Tension	50% torsion	70
OFHC Cu		
Test Mode	Prestrain	Cumulative $\bar{\epsilon}_p$ Level (%)
Compression	0	93
Torsion	0	100
Torsion	0	100
Compression/ Torsion	30% compression	100
Compression/Torsion	50% compression	100
Torsion/ Tension	50% torsion	55
6061-T6 Al		
Test Mode	Prestrain	Cumulative $\bar{\epsilon}_p$ Level (%)
Compression	0	50
Torsion	0	24
Torsion	0	50
Compression/ Torsion	30% Compression	80
Compression/ Torsion	60% Compression	90
Torsion/ Tension	10% Torsion	14

I.3 Data Files

Data for each of the aforementioned representative tests in Table 3 are available as ASCII data files on dos-formatted 3.5" floppy disks per request of D. L. McDowell. A brief description of each test is included at the top of each data file in the header information. All data file names are included in Table 4.

I.3.1. Pure Compression and Tension Following Torsion Tests

The header for compression and tension tests include the type of material, type of test, type of specimen used, and the nominal strain rate. In the case of tension tests, the torsional prestrain level is included. Data included in these files consists of the following two columns and in this order:

<div align="center">

True Stress (MPa)   True Strain

</div>

I.3.2. Pure Torsion and Prestrained Torsion Tests

The header at the top of the torsion data files includes the type of material, test type, nominal strain rate, prestrain history and level, and Lindholm specimen dimensions (gage length, inner and outer diameters in mm). Data included in these files consists of the following six columns and in this order:

Angle of Twist θ_g (radians)   Torque (N-m)   Shear Strain

Shear Stress (MPa)   Effective Plastic Strain   Effective Stress (MPa)

Table 4. Data File Names.

304L SS		
Test	$\bar{\sigma} - \bar{\epsilon}^p$ Data File	Axial Extension File
Compression	SSCOMP.ASC	
Torsion	SS00PT.ASC	SS00AX.ASC
30% Comp./Torsion	SS30CT.ASC	SS30AX.ASC
50% Comp./ Torsion	SS50CT.ASC	SS50AX.ASC
50% Torsion/Tension	SS50TT.ASC	
OFHC Cu		
Test	$\bar{\sigma} - \bar{\epsilon}^p$ Data File	Axial Extension File
Compression	CUCOMP.ASC	
Torsion	CU0PT1.ASC	CU0AX1.ASC
Torsion	CU0PT2.ASC	CU0AX2.ASC
30% Compr./ Torsion	CU30CT.ASC	CU30AX.ASC
50% Compr./Torsion	CU50CT.ASC	CU50AX.ASC
50% Torsion/ Tension	CU50TT.ASC	
6061-T6 Al		
Test	$\bar{\sigma} - \bar{\epsilon}^p$ Data File	Axial Extension File
Compression	ALCOMP.ASC	
Torsion	AL0PT1.ASC	AL0AX1.ASC
Torsion	AL0PT2.ASC	AL0AX2.ASC
30% Compr./ Torsion	AL30CT.ASC	AL30AX.ASC
60% Compr./ Torsion	AL60CT.ASC	AL60AX.ASC
10% Torsion/ Tension	AL10TT.ASC	

Companion axial extension data files the torsion and compression followed by torsion will consists of the following two columns

<u>Shear Strain</u>   <u>Axial Strain x1000</u>

I.4 Data Reduction

I.4.1. Torsion Tests

The following data reduction methodology was used for all torsion tests. Torque and angular displacements were converted to shear strain and shear stress via

$$\gamma = \frac{\bar{r}\,\theta_g}{l_g} \tag{1}$$

and

$$\tau = \frac{3\,T}{2\,\pi\,(r_o^{\,3} - r_i^{\,3})} \tag{2}$$

respectively. Here r_0 and r_i are the initial outer and inner diameter, θ_g is the angle of rotation of the top of the gage length relative to the bottom, l_g is the initial gage length for the specimen, and $\bar{r} = (r_0 + r_i)/2$. The von Mises uniaxial equivalent plastic strain and

stress are defined as

$$\bar{\epsilon}_p = \frac{(\dot{\gamma} - \tau/G)}{\sqrt{3}} \qquad \text{(3)}$$

and

$$\bar{\sigma} = \sqrt{3}\,\tau \qquad \text{(4)}$$

These equations were used to convert torque/ angle of twist data into von Mises equivalent plastic strain and stress. Elastic compliance corrections were applied to the data in order to correct for the elastic compliance of the material in the beveled region outside of the gage section, i.e.,

$$\theta_{measured} = \theta_{gage} + \theta_{compliance} \qquad \text{(5)}$$

where

$$\theta_{compliance} = CT \qquad \text{(6)}$$

Here, C is the compliance correction factor and T is the applied torque. Once C was found, equation (5) was used to find the corrected rotation of the gage section, θ_{gage}. These corrected values are presented in the torsion data files. Compliance correction factors were calculated as follows:

304L SS	1.36×10^{-6} /N-m

8

OFHC Cu 3.19×10^{-7} /N-m

6061-T6 Al 6.72×10^{-8} /N-m

I.4.2. Compression Tests

Compression test data were converted into axial engineering stress and axial engineering strain. From this, the true axial strain and true axial stress were calculated. The von Mises uniaxial equivalent plastic strain, for this case, is given by

$$\overline{\epsilon}_p = \epsilon_t - \frac{\sigma_t}{E} \tag{7}$$

where E is the Young's Modulus. No compliance corrections were needed for compression test specimens since an extensometer was used.

I.4.3. Tensile Tests

All tension tests were conducted on 2.0 Lindholm specimens after prestraining in torsion with no re-machining in-between test phases. An extensometer was mounted on the outside of the gage and bevel section of the specimen, so the total displacement across this 25.4 mm section was measured. Assuming that the bevel region remained elastic, its contribution to the deformation could be subtracted out using a linear compliance correction factor. Von Mises effective plastic strain was calculated according to equations (7).

9

Once again, a linear compliance correction factor was used in order to determine the difference between the measured displacement, Δl_m, and the displacement in the gage section, Δl_g, i.e.

$$\Delta l_m = \Delta l_g + KP \tag{8}$$

where Δl_m is the change in length measured by the extensometer and P is the applied load. Once K was found, equation (8) was used in order to calculate the actual displacement in the gage section. Compliance correction factors were calculated as follows:

304L SS	1.91×10^{-5} m/N
OFHC Cu	9.52×10^{-5} m/N
6061-T6 Al	1.74×10^{-5} m/N

MASTER COPY: PLEASE KEEP THIS "MEMORANDUM OF TRANSMITTAL" BLANK FOR REPRODUC-
TION PURPOSES. WHEN REPORTS ARE GENERATED UNDER ARO SPONSORSHIP, FORWARD A
COMPLETED COPY OF THIS FORM WITH EACH REPORT SHIPMENT TO THE ARO. THIS WILL
ASSURE PROPER IDENTIFICATION. **NOT TO BE USED FOR TECHNICAL PROGRESS REPORTS;**
SEE PAGE 4 PARA.(5) FOR PROGRESS REPORT INSTRUCTIONS.

MEMORANDUM OF TRANSMITTAL

U.S. Army Research Office
ATTN: AMXRO-RT-IPL (Hall)
P.O. Box 12211
Research Triangle Park, NC 27709-2211

____ Reprint (15 copies)   ____ Technical Report (40 copies)

____ Manuscript (1 copy)   __X__ Final Report (40 copies)

____ Thesis (1 copy)

____ MS   ____ PhD   ____ Other_____

CONTRACT/GRANT NUMBER ___DAAL 03-92-G-0103___

TITLE: ___A Critical Study of Constitutive Relations for Finite Strain Inelasticity___

is forwarded for your information.

SUBMITTED FOR PUBLICATION TO (applicable only if report is manuscript):

_____

_____

Sincerely,

David L. McDowell

DO NOT REMOVE THE LABEL BELOW
THIS IS FOR IDENTIFICATION PURPOSES

Dr. David L. McDowell   29543-EG
Georgia Institute of Technology   ·13·
Department of Mechanical Engineering
Atlanta, GA 30332